DESIGN OF NETWORKS WITH MULTIPLE OAs AND OTAs USING BETA MATRICES

by

Sadik Esmelioglu

Bachelor of Science
Bogazici University, 1980

Master of Science
University of South Carolina, 1982

Submitted in Partial Fulfillment of the Requirements

for the Degree of Doctor of Philosophy in the

Department of Electrical and Computer Engineering

University of South Carolina

1986

Major Professor

Committee Member

Chairman, Examining Committee

Committee Member

Dean of the Graduate School

TABLE OF CONTENTS

ACKNOWLEDGEMENTS

The author wishes to acknowledge with gratitude the invaluable assistance and guidance provided by Dr. G.M. Wierzba as an advisor, a teacher, and a friend under whose supervision this dissertation has been written.

The works of many authors which have inspired and provided a basis for this work are also appreciated and acknowledged.

DESIGN OF NETWORKS WITH MULTIPLE OAs AND OTAs
USING BETA MATRICES

by

SADIK ESMELIOGLU

ABSTRACT

Operational Amplifiers (OAs) and Operational Transconductance Amplifiers (OTAs) are basic building blocks widely used in the design of active networks. Because of their nonideal parameters, especially the frequency dependent open-loop gain, the design of networks containing these devices has been cumbersome.

A method is presented which separates these frequency dependent building blocks from the rest of the network. The latter is treated as a complex feedback network. This feedback network is described by a matrix called the beta matrix whose diagonal entries represent the self feedback of each block, while the off-diagonal entries represent the loading effects between the blocks.

Using this concept of feedback, the derivation of the transfer function, stability, and sensitivity analyses of such networks are introduced. Also, some design considerations are presented.

From a network containing multiple OAs a set of networks can be generated, all of which have identical ideal gain expressions. This idea is called the "OA Relocation". Using the beta matrix method, it is possible to select the networks with better performance. Practical examples are given to demonstrate the beta matrix method and its use as a design tool.

I. BACKGROUND AND PREVIEW

1.1 Introduction

The purpose of this chapter is to provide background information on the theory of active networks using Operational Amplifiers (OAs) and Operational Transconductance Amplifiers (OTAs). Also in this chapter, some of the results introduced in this dissertation are previewed.

1.2 Background

The analysis of active networks with feedback requires the determination of the transfer function, input and output impedances, stability, and sensitivity. A number of methods have been proposed in the literature for this purpose. The value of a method is measured by its completeness, ease of application and the amount of comprehensive information it supplies to the designer. Using these evaluation criteria, a discussion of the presently available methods follows.

On the determination of the transfer function, input and output impedances, the classical approach has been and still is the educational tool. This approach which is introduced in many textbooks, such as by Sedra and Smith [1], requires the identification of the feedback, its topology and the loading effects. This method allows only a single amplifier and a single feedback loop. Simpler methods have been proposed by Rosenstark [2], Davis [3], and Esmelioglu [4], for single amplifier configurations. Eventhough the single amplifier case plays a significant role in the active network theory, there is still need for an extended theory - since the usage of building blocks (like OAs and OTAs) connected through a mesh of feedback loops has become a common design practice. Among the methods which can handle multiple-amplifier cases, the Modified Nodal Analysis (MNA), proposed by Ho [5], is very easy to apply. However, the size of the matrix describing the network is too big to derive any comprehensive information. Another easy to follow method is introduced by Wilson [6]. Unfortunately, the open-loop gains of the OAs are embedded in the transfer function. To obtain the ideal gain, extra operations are needed. Moreover, this approach is not suitable for determining the input and output impedance expressions. The technique used by Geiger in [7], although very similar to the one presented in the next chapter, is aimed at the analysis of active filters containing one to three OAs. That is, the method is not generalized; nor does it provide the input and output impedance analysis. The beta network approach proposed by Esmelioglu in [8], which is a basis for this dissertation, makes use of sub-network transfer functions to determine the overall transfer function, input and output impedances. However, as the number of OAs increases, the task of determining the sub-network transfer functions becomes cumbersome.

On the determination of stability, most of the recent work has been done in the field of control theory [9]-[14]. A survey by MacFarlane [11], summarizes some of the recent work on the linear multivariable feedback theory. Since the system equations introduced in Chapter 1 of this dissertation are similar to those describing control systems, some of the concepts (such as the eigenvalue problem and diagonal dominance) can be adapted to network theory. Some traditional techniques like Nyquist criterion, Bode plots, and Routh-Hurwitz test can be used to determine the stability. However, because of the vast number of possible variables in larger networks, these techniques are inefficient to employ. In a recent paper [15], Geiger proposes a technique to approximate the location of the parasitic poles. These poles are introduced by the OAs and can make the network unstable, if they are found to be in the right half of the complex plane (RHP). This method is a great improvement over the actual determination of the system poles. However, the information about what may be causing instability is lost in the required calculations.

On the subject of active sensitivity, most of the work in the literature has been directed towards second order active filters. The method presented by Wilson [16] is an excellent approximation for low frequency designs. It also suggests a design technique to minimize the active sensitivity. Mackay has introduced a numerical sensitivity minimization technique in [17]. His method uses a sensitivity performance measure to minimize the sensitivity of state-space active filters. Another technique devised by Mikhael in [18], approximates the denominator by a second order polynomial to determine the sensitivities. The results, however, are similar to that obtained by Wilson in [16]. A series of two papers by Geiger, [7] and [19], outlines a technique to obtain active filters with zero amplifier sensitivity. Geiger makes use of Maclaurin series expansion of the denominator to determine the changes in the ideal poles due to the time constant of the OAs. The same series expansion method will be used in this dissertation to determine not only the changes in the ideal poles, but also the changes in the ideal zeros due to the gain-bandwidth product (GB) of the OAs.

A network consists of passive components and active building blocks.

The active building blocks introduce some constraints on the passive network. Antoniou in [20] showed that new networks with the same ideal characteristics can be obtained. This is accomplished by changing the active component connections while keeping the same original passive component connections. This concept has been extended by Palomera-Garcia [21] and Wierzba [22].

The most commonly used building block in active network design is the OA, a voltage-controlled voltage-source. An OTA, a voltage-controlled current-source, is another building block which is becoming popular, especially in voltage-tunable filter applications. Some of these applications can be found in [23]-[25].

1.3 Preview

In Chapter 2, a method is developed to derive the expressions for the voltage transfer function, input and output impedances of an n-OA network a network employing n OAs. The network is divided into two parts: i) The active components (OAs) and ii) The passive network, which is viewed as the feedback network. Then the system equations are written relating the output of the network and the inputs of the OAs to the input of the network and the outputs of the OAs. These equations resemble the state and output equations for a control system where the outputs of the OAs are taken as the state variables.

In Chapter 3, the stability of n-OA networks is studied. First, a general stability criterion is stated using the eigenvalue method. Then, some special cases are considered; special cases like the feedback structures resulting in diagonal, triangular, or diagonally dominant matrices. If a network falls into one of these catagories, then the n-OA stability problem can be reduced to n 1-OA stability problems. Finally, in this chapter, an easy stability test is presented. This test (High Frequency Stability Test) imposes some necessary but not sufficient conditions on the OAs. Another type of instability is also observed due to the movements of the ideal poles. This topic is treated in detail in the sensitivity chapter.

In Chapter 4, the active sensitivity of n-OA networks is examined. The active sensitivity is the change in the ideal design parameters due to the finite GB of the OAs. The expressions for calculating the active sensitivities of the ideal poles and zeros of the network are derived using the Maclaurin series approximation. In addition to the general expressions where the OAs may have different GBs, simpler expressions are also derived assuming matched OAs.

In Chapter 5, methods to generate new networks with the same ideal gain are presented. Given an n-OA network, it is possible to obtain other networks by relocating the OA connections. This process is called OA Relocation. There are two types of OA Relocation: a) Output relocation, and b) Input relocation. These relocation techniques and how they modify the system matrices are introduced in this chapter. Also in this chapter, another method, called the Voltage Divider Method will be presented. The Voltage Divider Method, which modifies the input port of the OA, is used to improve the high frequency stability of a network. This is demonstrated in the applications chapter.

In Chapter 6, the ideal and nonideal characteristics of the OTA are discussed. Also, the voltage transfer function, input and output impedance expressions for n-OTA networks are derived using methods presented in Chapter 2. Stability and sensitivity considerations for n-OTA networks are also included in this chapter.

In Chapter 7, some of the methods developed in the preceeding chapters are applied to two existing active filters. First, a step-by-step analysis procedure is suggested. Then, using this procedure the performance of the two filters and other filters generated from them are calculated and compared.

In Chapter 8, a summary of the results obtained along with some problems for future research are given.

II. NETWORKS CONTAINING n-OAs

2.1 Introduction

In this chapter, first, the ideal and the non-ideal characteristics of the Operational Amplifier (OA) are introduced. Then, in subsequent theorems, the general expressions for the voltage gain, input and output impedances of n-OA networks are presented.

2.2 Operational Amplifier

The OA is basically a difference amplifier with a high input and a low output impedance, and a very high DC open-loop voltage gain. The circuit symbol and a model for the OA is shown in Figure 2.2.1. It should be noted that the polarity of the input voltage is chosen opposite to that of the amplifier polarity. This choice of signs is made to eliminate the negative signs from the network equations, as will be apparent later in this chapter.

Ideally, the voltage gain, A, the input impedance, r_i, are infinite, and the output impedance, r_o, is zero. The finite r_i and nonzero r_o of the real OA have little effect in most of the applications. However, if it is desired to include these impedances in the analysis, they may be shown externally, as in Figure 2.2.2. In the examples studied here, r_i and r_o will be omitted and the open-loop gain, A will be considered as the only non-ideal parameter of the OA.

For a real OA, the open-loop gain, A, is not only finite, but has also a frequency response. The manufacturer supplies the experimental frequency

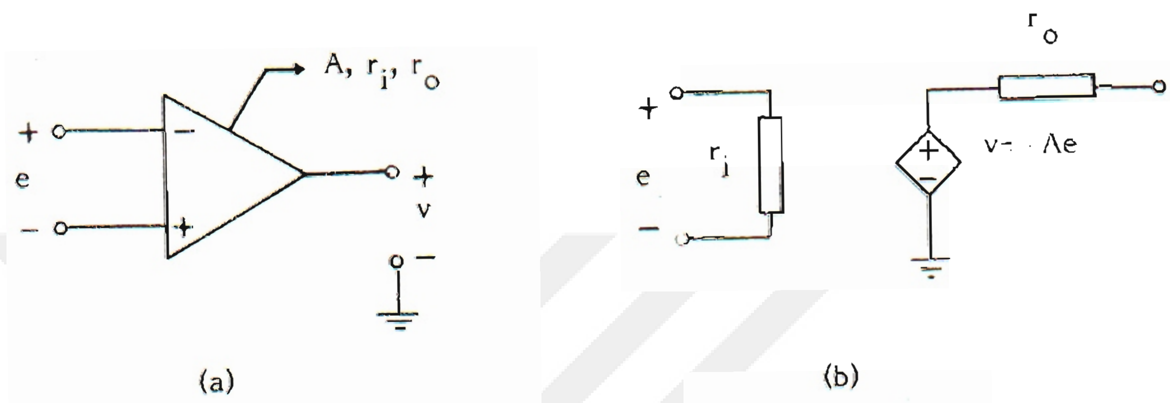

Figure 2.2.1 Operational Amplifier, (a) Circuit Symbol, (b) Model

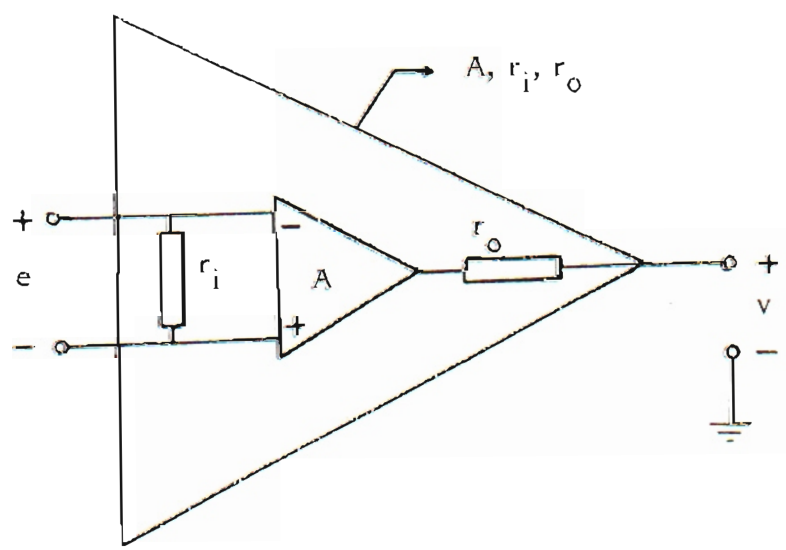

Figure 2.2.2 OA with r_i and r_o shown externally

response of A in the form of Bode plots. However, A is frequently approximated analytically by a two pole model as shown in equation 2.2.1.

$$A = \frac{A_o}{(1+\frac{s}{\omega_L})(1+\frac{s}{\omega_H})} = \frac{kGB^2}{(s+\omega_L)(s+kGB)} \qquad (2.2.1)$$

Where A_o is the DC gain (typically 200,000), ω_L is the low frequency pole (typically f_L=5Hz), ω_H is the high frequency pole (typically f_H=7MHz). As shown in the second part of equation 2.2.1, the open-loop gain is generally characterized by its gain-bandwidth product, GB ($A_o\,\omega_L$=GB and ω_H=kGB where k is a constant which determines the location of the high frequency pole). Further approximations are also used depending on the range of signal frequencies applied. These approximations are shown in equations 2.2.2 - 2.2.5.

$$A = A_o \qquad \text{for } \omega << \omega_L \quad \text{(DC)} \qquad (2.2.2)$$

$$A = \frac{GB}{s+\omega_L} \qquad \text{for } \omega << \omega_H \qquad (2.2.3)$$

$$A = \frac{GB}{s} \qquad \text{for } \omega_L << \omega << \omega_H \qquad (2.2.4)$$

$$A = \frac{kGB^2}{s(s+kGB)} \qquad \text{for } \omega >> \omega_L \qquad (2.2.5)$$

There are a number of other non-ideal parameters, like slew-rate, common-mode rejection ratio, maximum swing, etc. However, the majority of the problems in an OA network are caused by the finite and frequency dependent open-loop gain.

2.3 Transfer Function

Theorem 2.3.1 stated below describes the general form of the transfer function for an n-OA network.

Theorem 2.3.1: Given an n-OA network as shown in Figure 2.3.1, the transfer function is of the form of equation 2.3.1.

$$T(s) = \frac{V_o}{V_{in}} = \zeta - \alpha(A^{-1} + \beta)^{-1}\gamma = \frac{\det \begin{bmatrix} A^{-1}+\beta & \gamma \\ \alpha & \zeta \end{bmatrix}}{\det\ (A^{-1} + \beta)} \tag{2.3.1}$$

where

$$A^{-1} = \mathrm{diag}\left(\frac{1}{A_1}, \ldots, \frac{1}{A_n}\right) \tag{2.3.2}$$

$$\beta = [\beta_{ij}]_{n\times n}, \quad \beta_{ij} = \left.\frac{e_i}{v_j}\right|_{\substack{v_k = V_{in} = 0 \\ k \neq j}} \tag{2.3.3}$$

$$\gamma = [\gamma_i]_{n\times 1}, \quad \gamma_i = \left.\frac{e_i}{V_{in}}\right|_{v_j = 0 \quad j = 1,\ldots,n} \tag{2.3.4}$$

$$\alpha = [\alpha_j]_{1\times n}, \quad \alpha_j = \left.\frac{V_o}{v_j}\right|_{\substack{v_k = V_{in} = 0 \\ k \neq j}} \tag{2.3.5}$$

$$\zeta = [\zeta]_{1\times 1}, \quad \zeta = \left.\frac{V_o}{V_{in}}\right|_{v_j = 0 \quad j = 1,\ldots,n} \tag{2.3.6}$$

Proof: Remembering that the OAs in Figure 2.3.1 do not draw any current from the feedback network, each OA input, e_i, and the network output, V_o, can be expressed in terms of the OA outputs, v_j, and the network input, V_{in}, using superposition:

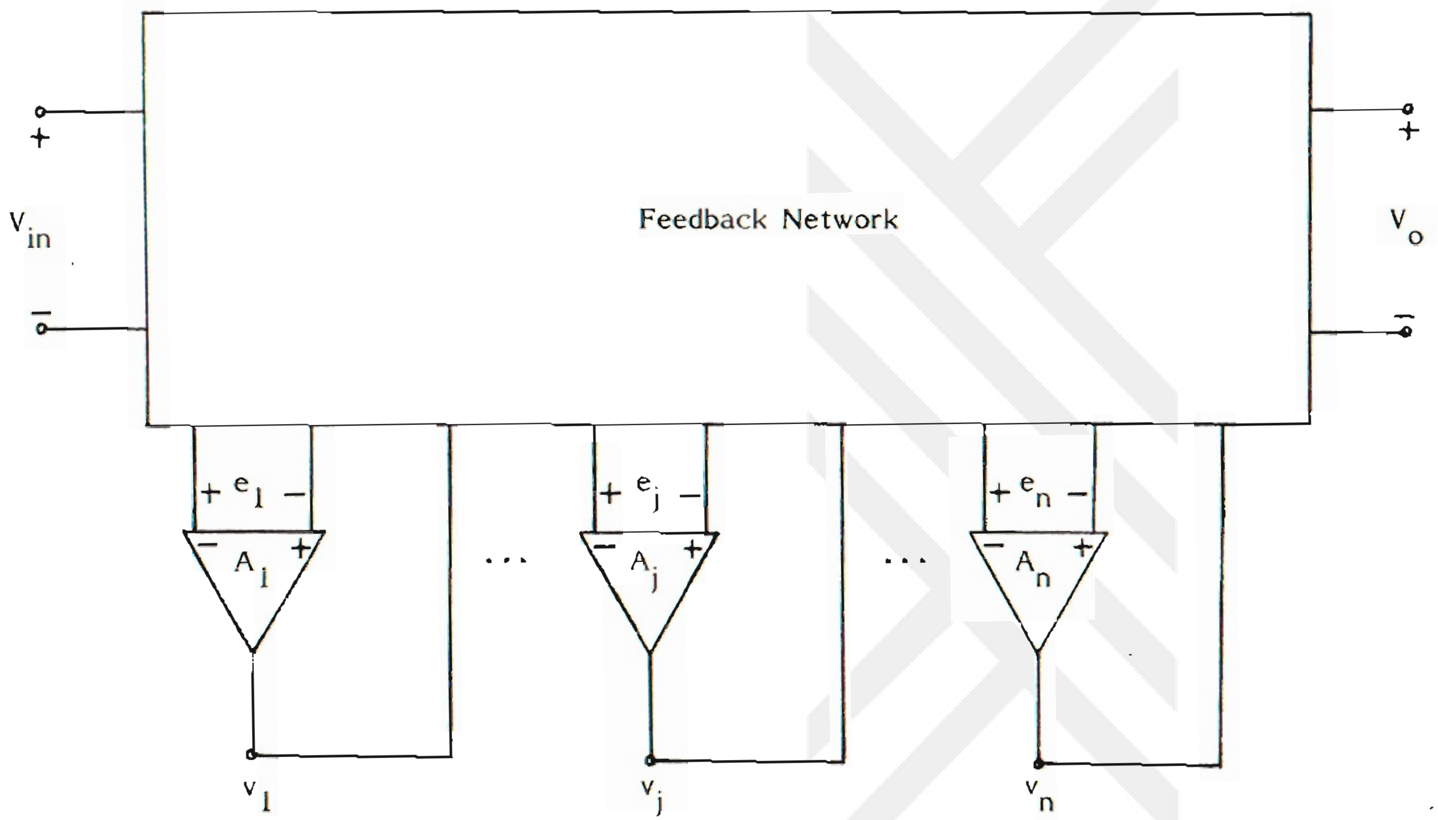

Figure 2.3.1 An n-OA network

$$
\begin{aligned}
e_1 &= h_{11}v_1+\dots+h_{1n}v_n + p_1\, V_{in} \\
&\ \vdots \\
e_n &= h_{n1}v_1+\dots+h_{nn}v_n + p_n\, V_{in} \\
V_o &= q_1 v_1 +\dots+q_n v_n + r\, V_{in}
\end{aligned}
\tag{2.3.7}
$$

or in matrix form,

$$
\begin{aligned}
e &= Hv + P\, V_{in} \\
V_o &= Qv + R\, V_{in}
\end{aligned}
\tag{2.3.8}
$$

where

$$e = [e_1 \dots e_n]^T \quad , \quad v = [v_1 \dots v_n]^T$$

and

$$H = [h_{ij}]_{nxn} \quad , \quad h_{ij} = \frac{e_i}{v_j}\Bigg|_{\substack{v_k = V_{in} = 0 \\ k \neq j}} \tag{2.3.9}$$

$$P = [p_i]_{nx1} \quad , \quad p_i = \frac{e_i}{V_{in}}\Bigg|_{v_j = 0 \quad j = 1,\dots,n} \tag{2.3.10}$$

$$Q = [q_j]_{1xn} \quad , \quad q_j = \frac{V_o}{v_j}\Bigg|_{\substack{v_k = V_{in} = 0 \\ k \neq j}} \tag{2.3.11}$$

$$R = [r] \quad , \quad r = \frac{V_o}{V_{in}}\Bigg|_{v_j = 0 \quad j = 1,\dots,n} \tag{2.3.12}$$

Comparing equations 2.3.3-2.3.6 to equations 2.3.9-2.3.12, it is seen that, $H = \beta$, $P = \gamma$, $Q = \alpha$, and $R = \zeta$. Then equation 2.3.8 becomes

$$e = \beta v + \gamma V_{in}$$
$$V_o = \alpha v + \zeta V_{in} \qquad (2.3.13)$$

Also, it is known that the input of an OA is related to its output by

$$e_i = -\frac{1}{A_i} v_i$$

or in matrix form

$$e = -A^{-1} v \qquad (2.3.14)$$

Now, manipulating equations 2.3.13 and 2.3.14, the transfer function, T(s), can be expressed as

$$T(s) = \frac{V_o}{V_{in}} = \zeta - \alpha (A^{-1} + \beta)^{-1} \gamma$$

which proves one side of equation 2.3.1. To prove the other side, equation 2.3.14 is inserted in equation 2.3.13, resulting in

$$0 = (A^{-1} + \beta) v + \gamma V_{in}$$
$$V_o = \alpha v + \zeta V_{in} \qquad (2.3.15)$$

Now, applying the Cramer's rule to equation 2.3.15, the transfer function can be obtained as below

$$T(s) = \frac{V_o}{V_{in}} = \frac{\det \begin{bmatrix} A^{-1} + \beta & \gamma \\ \alpha & \zeta \end{bmatrix}}{\det(A^{-1} + \beta)}$$

Thus, the theorem is proved.

It is interesting to note that the equation 2.3.13, which will be referred to as the system equations, resembles the state and the output equations of a single-input-single-output (SISO) control system, where the outputs of the OAs, v_i, are observed as the state variables. The system equations can be modified to represent a multi-input-multi-output (MIMO) network without any major changes.

Corollary 2.3.1: The ideal gain of an n-OA network is given by equation 2.3.16.

$$K(s) = B'/B \tag{2.3.16}$$

where

$$B = \det(\beta)$$

and

$$B' = \det\begin{bmatrix} \beta & \gamma \\ \alpha & \zeta \end{bmatrix}$$

Proof: The ideal gain of an n-OA network is found by letting all OAs be ideal, that is A_i goes to infinity (or $1/A_i$ goes to zero). Then, the open-loop gain matrix

$$\lim_{A_i \to \infty} [A^{-1} = \mathrm{diag}(\frac{1}{A_1},\ldots,\frac{1}{A_n})] = 0$$

Thus, from equation 2.3.1

$$K(s) = \lim_{A_i \to \infty} T(s) = \frac{\det\begin{bmatrix} \beta & \gamma \\ \alpha & \zeta \end{bmatrix}}{\det(\beta)}$$

2.4 Input Impedance

The method to obtain the input impedance of an n-OA network is outlined in the theorem stated below.

Theorem 2.4.1: Given an n-OA network as shown in Figure 2.4.1, the input impedance, $Z_{in}(s)$, is given by equation 2.4.1.

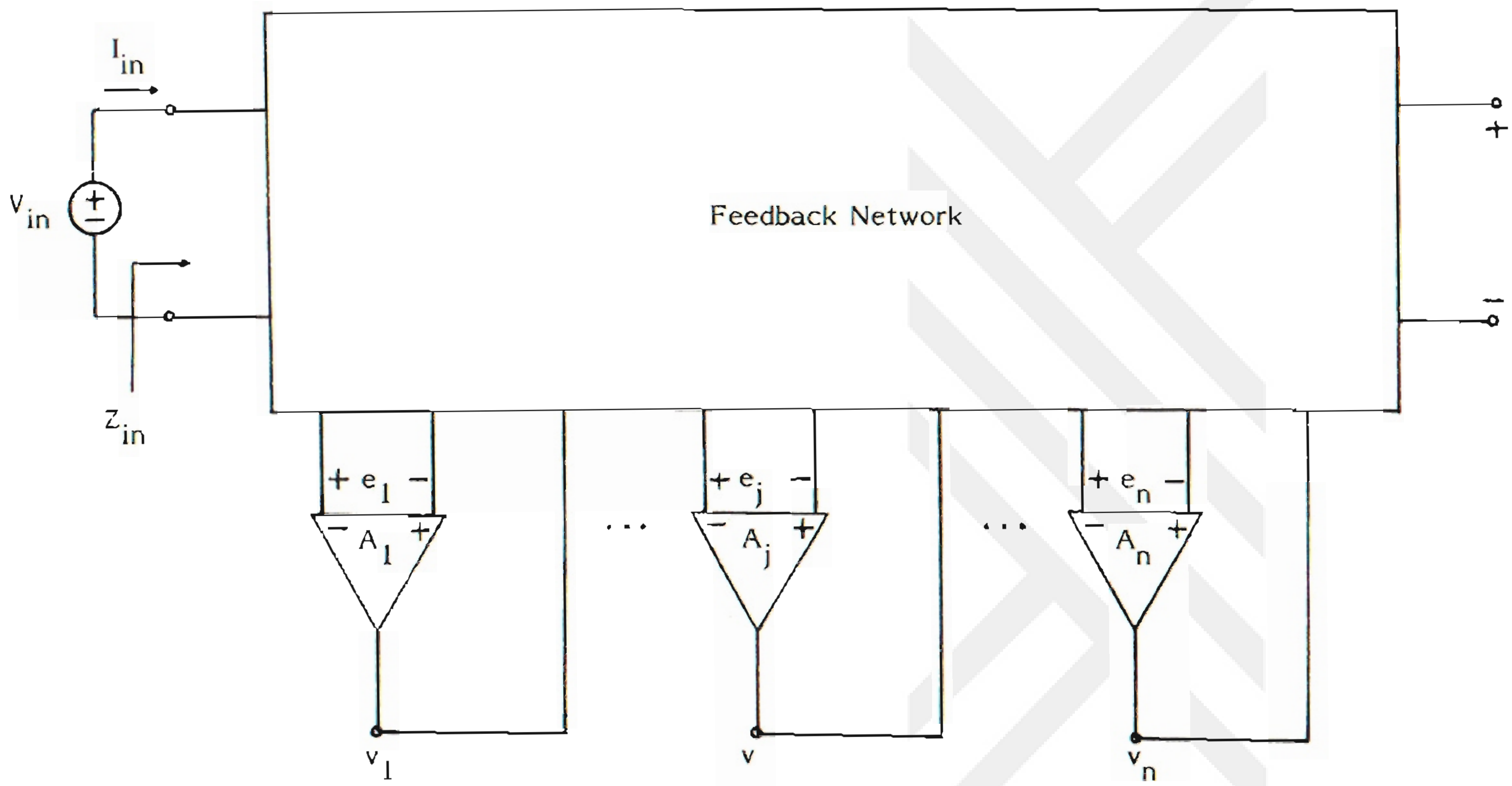

Figure 2.4.1 The n-OA network to determine Z_{in}

$$Z_{in}(s) = \frac{V_{in}}{I_{in}} = \frac{1}{\zeta^{oc} - \alpha^{oc}(A^{-1} + \beta)^{-1}\,\gamma} = \frac{\det(A^{-1} + \beta)}{\det\begin{bmatrix} A^{-1} + \beta & \gamma \\ \alpha^{oc} & \zeta^{oc} \end{bmatrix}} \qquad (2.4.1)$$

where A^{-1}, β , and γ are as described in equations 2.3.2, 2.3.3, and 2.3.4 respectively, and

$$\alpha^{oc} = [\alpha_j]_{1xn} \quad , \quad \alpha_j^{oc} = \frac{I_{in}}{v_j}\Bigg|_{\substack{v_k = V_{in} = 0 \\ k \neq j}} \qquad (2.4.2)$$

$$\zeta^{oc} = [\zeta^{oc}]_{1x1} \quad , \quad \zeta^{oc} = \frac{I_{in}}{V_{in}}\Bigg|_{v_j = 0 \qquad j = 1,\ldots,n} \qquad (2.4.3)$$

Proof: The proof of this theorem is similar to the proof of Theorem 2.3.1, the only difference is that the output variable is I_{in}, instead of V_o, i.e. the system equations for the input impedance are written as

$$\begin{aligned} e &= \beta v + \gamma\, V_{in} \\ I_{in} &= \alpha^{oc} v + \zeta^{oc} V_{in} \end{aligned} \qquad (2.4.4)$$

Corollary 2.4.1: The ideal input impedance of an n-OA network can be expressed as

$$Z_{in_o}(s) = B/B^{oc} \qquad (2.4.5)$$

where

$$B = \det(\beta)$$

and

$$B^{oc} = \begin{bmatrix} \beta & \gamma \\ \alpha^{oc} & \zeta^{oc} \end{bmatrix}$$

Proof: The ideal input impedance is derived by assuming ideal OAs. Thus, A^{-1} becomes a zero matrix and from equation 2.4.1,

$$Z_{in_o}(s) = \lim_{A_i \to \infty} Z_{in}(s) = \frac{\det(\beta)}{\det \begin{bmatrix} \beta & \gamma \\ \alpha^{oc} & \zeta^{oc} \end{bmatrix}}$$

2.5 Output Impedance

The output impedance of an n-OA network as given in Figure 2.3.1, is determined by shorting the network input terminals, applying a test current at the output port, and calculating the resulting voltage across the current source (Figure 2.5.1).

The following theorem states the general expression for the output impedance.

Theorem 2.5.1: Referring to Figure 2.5.1, the output impedance, $Z_{out}(s)$, of an n-OA network is given by the following equation:

$$Z_{out}(s) = \zeta^{sc} - \alpha\,(A^{-1} + \beta)^{-1}\,\gamma^{sc} = \frac{\det \begin{bmatrix} A^{-1} + \beta & \gamma^{sc} \\ \alpha & \zeta^{sc} \end{bmatrix}}{\det(A^{-1} + \beta)} \qquad (2.5.1)$$

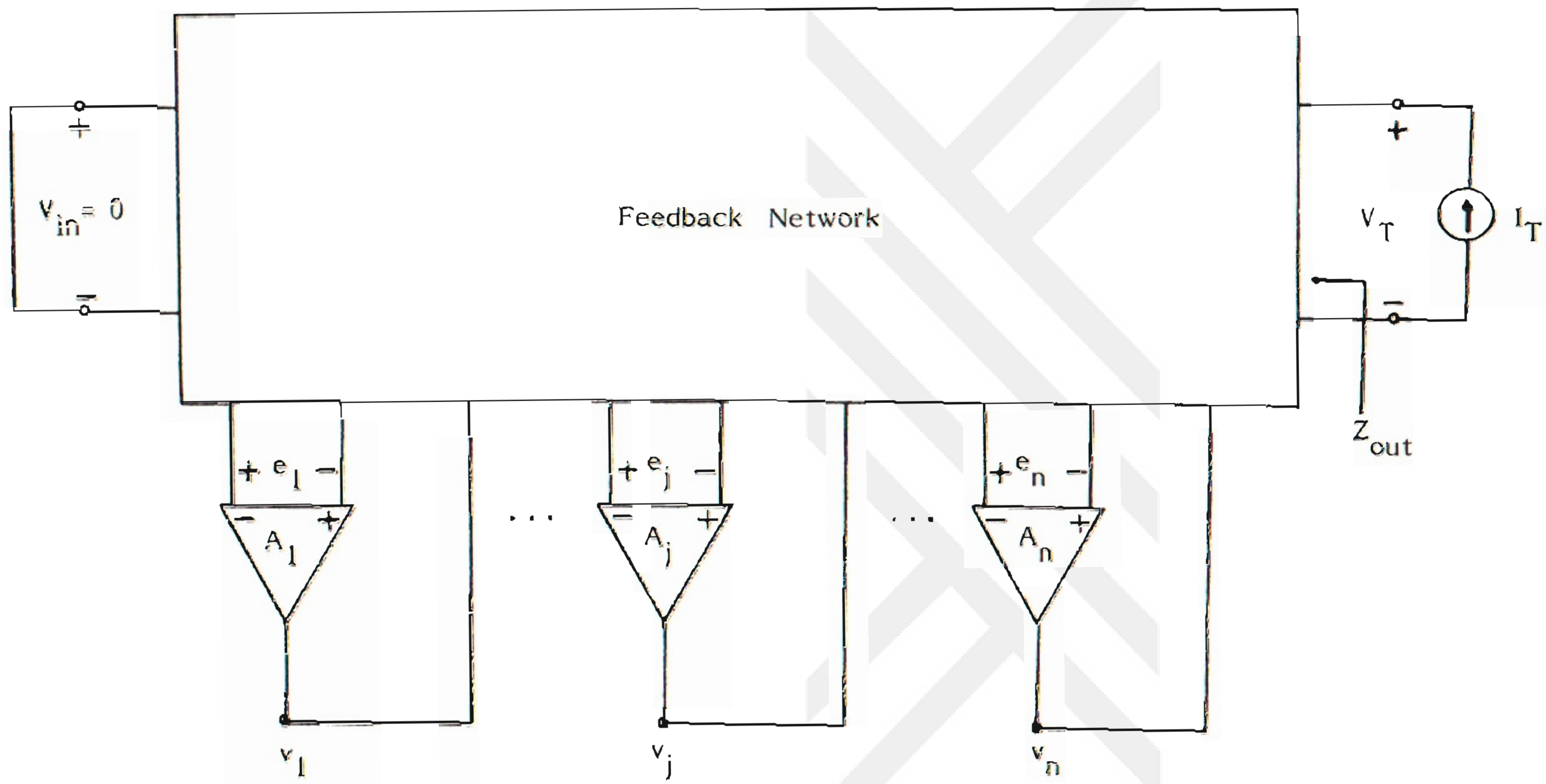

Figure 2.5.1 The network to determine Z_{out}

where A^{-1}, β, and α are given by equations 2.3.2, 2.3.3, and 2.3.5, respectively, and

$$\gamma^{sc} = [\gamma_i^{sc}]_{nx1} \quad , \quad \gamma_i^{sc} = \frac{e_i}{I_T} \Bigg| \; v_j = V_{in} = 0 \quad j = 1,\ldots,n \tag{2.5.2}$$

$$\zeta^{sc} = [\zeta^{sc}]_{1x1} \quad , \quad \zeta^{sc} = \frac{V_T}{I_T} \Bigg| \; v_j = V_{in} = 0 \quad j = 1,\ldots,n \tag{2.5.3}$$

Proof: The proof of this theorem is similar to the proof of Theorem 2.3.1. Comparing Figure 2.5.1 to Figure 2.3.1, the input to the network of Figure 2.5.1 is I_T, and the output is V_T. Thus, the system equations for the output impedance can be written as

$$\begin{aligned} e &= \beta v + \gamma^{sc} I_T \\ V_T &= \alpha v + \zeta^{sc} I_T \end{aligned} \tag{2.5.4}$$

The matrices β and α are the same as the ones described in Theorem 2.3.1, since in determining the entries of these matrices, I_T is set to zero, that is the output terminals are opened.

Corollary 2.5.1: The ideal output impedance of an n-OA network is given by

$$Z_{out_o}(s) = B^{sc}/B \tag{2.5.5}$$

where

$$B = \det(\beta)$$

and

$$B^{sc} = \det \begin{bmatrix} \beta & \gamma^{sc} \\ \alpha & \zeta^{sc} \end{bmatrix}$$

Proof: Similar to the proofs of the previous corollaries, letting A_i go to infinity, equation 2.5.5 can be obtained from equation 2.5.1.

2.6 Examples

As an illustration of the methods outlined in the preceeding theorems, consider the following two examples.

Example 2.6.1: The network of Figure 2.6.1 is commonly known as the Kerwin-Huelsman-Newcomb (KHN) filter [26]. The gain, input and output impedance expressions for the KHN filter are derived below.

Gain:

$$\beta = \begin{bmatrix} k_1 & -k_2 & k_3 \\ \frac{\omega_1}{D_1} & \frac{s}{D_1} & 0 \\ 0 & \frac{\omega_2}{D_2} & \frac{s}{D_2} \end{bmatrix} \qquad \begin{matrix} \gamma = [-k_4 \quad 0 \quad 0\,]^T \\ \alpha = [\,0 \quad 1 \quad 0\,] \\ \zeta = [\,0\,] \end{matrix}$$

where $D_1 = (s + \omega_1)$, $D_2 = (s + \omega_2)$,

$$k_1 = \frac{G_6}{G_5+G_6},\ k_2 = \frac{G_4}{G_3+G_4},\ k_3 = \frac{G_5}{G_5+G_6},\ k_4 = \frac{G_3}{G_3+G_4},\ \omega_1 = \frac{G_1}{C_1},\ \text{and}\ \omega_2 = \frac{G_2}{C_2}$$

$$T(s) = \frac{X(s)}{Y(s)}$$

where

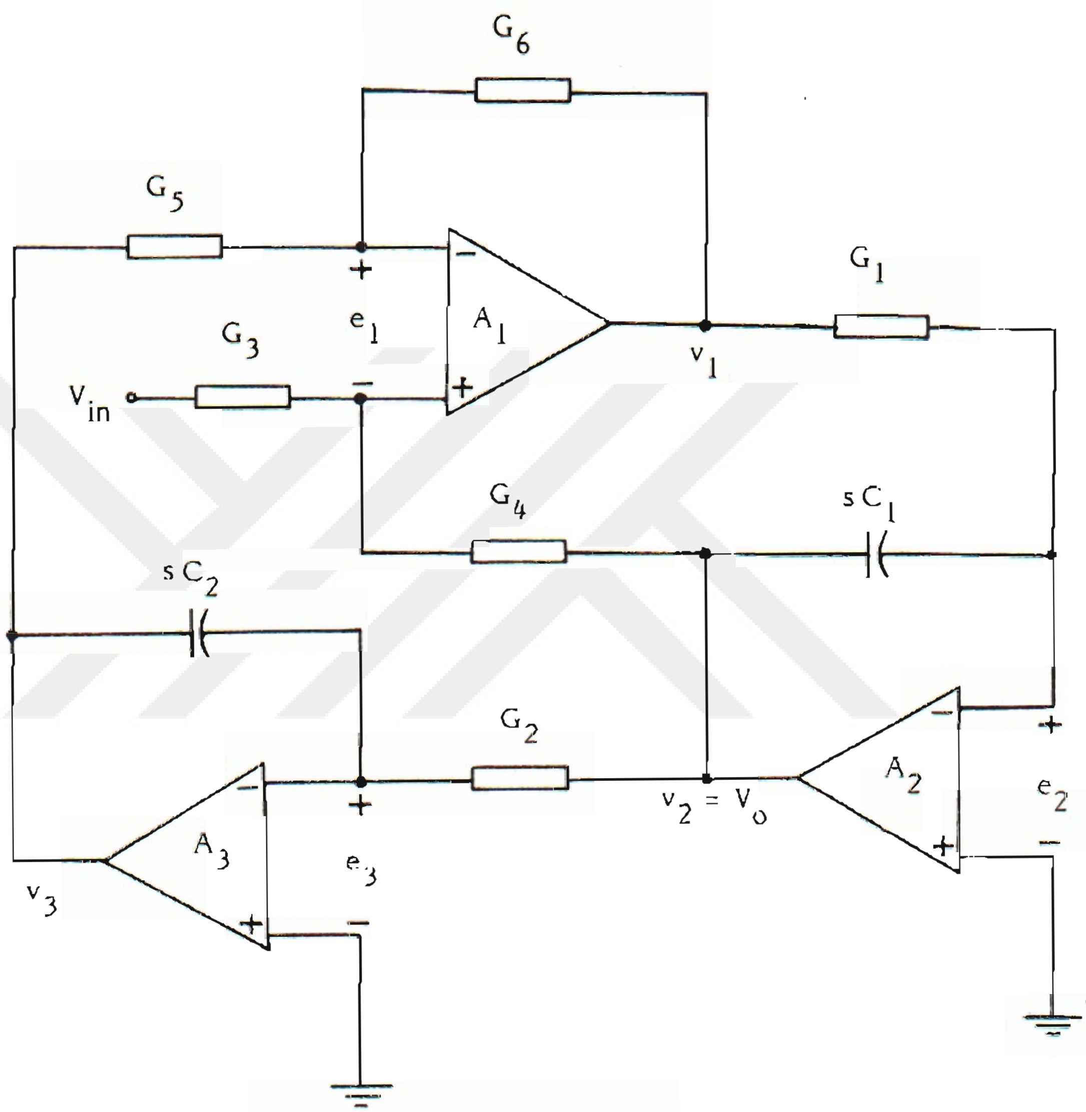

Figure 2.6.1 The KHN Filter

$$X(s) = \det \begin{bmatrix} A^{-1}+\beta & \gamma \\ \alpha & \zeta \end{bmatrix} = -\frac{1}{A_3} k_4 \frac{\omega_1}{D_1} - k_4 \frac{\omega_1}{D_1}\frac{s}{D_2}$$

$$Y(s) = \det (A^{-1}+\beta) = \frac{1}{A_1A_2A_3} + \frac{1}{A_1A_2}\frac{s}{D_1} + \frac{1}{A_1A_3}\frac{s}{D_2} + \frac{1}{A_2A_3} k_1$$

$$+\frac{1}{A_1}\frac{s}{D_1}\frac{s}{D_2} + \frac{1}{A_2} k_1 \frac{s}{D_2} + \frac{1}{A_3} \frac{k_1 s + k_2 \omega_1}{D_1}$$

$$+ \frac{k_1 s^2 + k_2 \omega_1 s + k_3 \omega_1 \omega_2}{D_1 D_2}$$

and the ideal gain is

$$K(s) = \frac{-k_4 \omega_1 s}{k_1 s^2 + k_2 \omega_1 s + k_3 \omega_1 \omega_2}$$

Input Impedance:

$$\alpha^{oc} = [\,0 \quad -k_5 \quad 0\,] \quad \text{and} \quad \zeta^{oc} = [k_5]$$

where $k_5 = \dfrac{G_3G_4}{G_3+G_4}$

$$Z_{in}(s) = \frac{Y(s)}{X^{oc}(s)}$$

$$X^{oc}(s) = \frac{1}{A_1A_2A_3} k_5 + \frac{1}{A_1A_2} k_5 \frac{s}{D_2} + \frac{1}{A_1A_3} k_5 \frac{s}{D_1} + \frac{1}{A_2A_3} k_1 k_5$$

$$+ \frac{1}{A_1} k_5 \frac{s}{D_1}\frac{s}{D_2} + \frac{1}{A_2} k_1 k_5 \frac{s}{D_2} + \frac{1}{A_3} k_5 \frac{k_1 s + (k_2+k_4)\,\omega_1}{D_1}$$

$$+ k_5 \frac{k_1 s + (k_2+k_4)\,\omega_1 s + k_3 \omega_1 \omega_2}{D_1 D_2}$$

and the ideal gain is

$$Z_{in_o}(s) = \frac{1}{k_5}$$

Output Impedance:

$$Y^{sc} = [\ 0\ 0\ 0\ ]^T \qquad \zeta^{sc} = [\ 0\ ]$$

Thus, $$Z_{out}(s) = Z_{out_o}(s) = 0$$

Example 2.6.2: The network of Figure 2.6.2 is called the Generalized-Immittance Converter (GIC) [27] and is mostly used to simulate an inductor. The input impedance expression is derived below.

$$\beta = \begin{bmatrix} h_1 & h_2 \\ (h_1 - h_3) & h_2 \end{bmatrix} \qquad \begin{matrix} \alpha = [-1 \quad 0]^T \\ \alpha^{oc} = [0 \quad -Y_1] \end{matrix} \qquad \zeta^{oc} = [Y_1]$$

where $$h_1 = \frac{Y_3}{Y_2+Y_3},\ h_2 = \frac{Y_2}{Y_2+Y_3},\ \text{and}\ h_3 = \frac{Y_4}{Y_4+Y_L}$$

Then, $$Z_{in}(s) = \frac{Y(s)}{X^{oc}(s)} \quad \text{where}$$

$$Y(s) = \frac{1}{A_1 A_2} + \frac{1}{A_1} h_2 + \frac{1}{A_2} h_1 + h_2 h_3$$

$$X^{oc}(s) = Y_1 \left[\frac{1}{A_1 A_2} + \frac{1}{A_1} h_1 + h_1 (1 - h_3)\right]$$

Ideally, the input impedance is given by

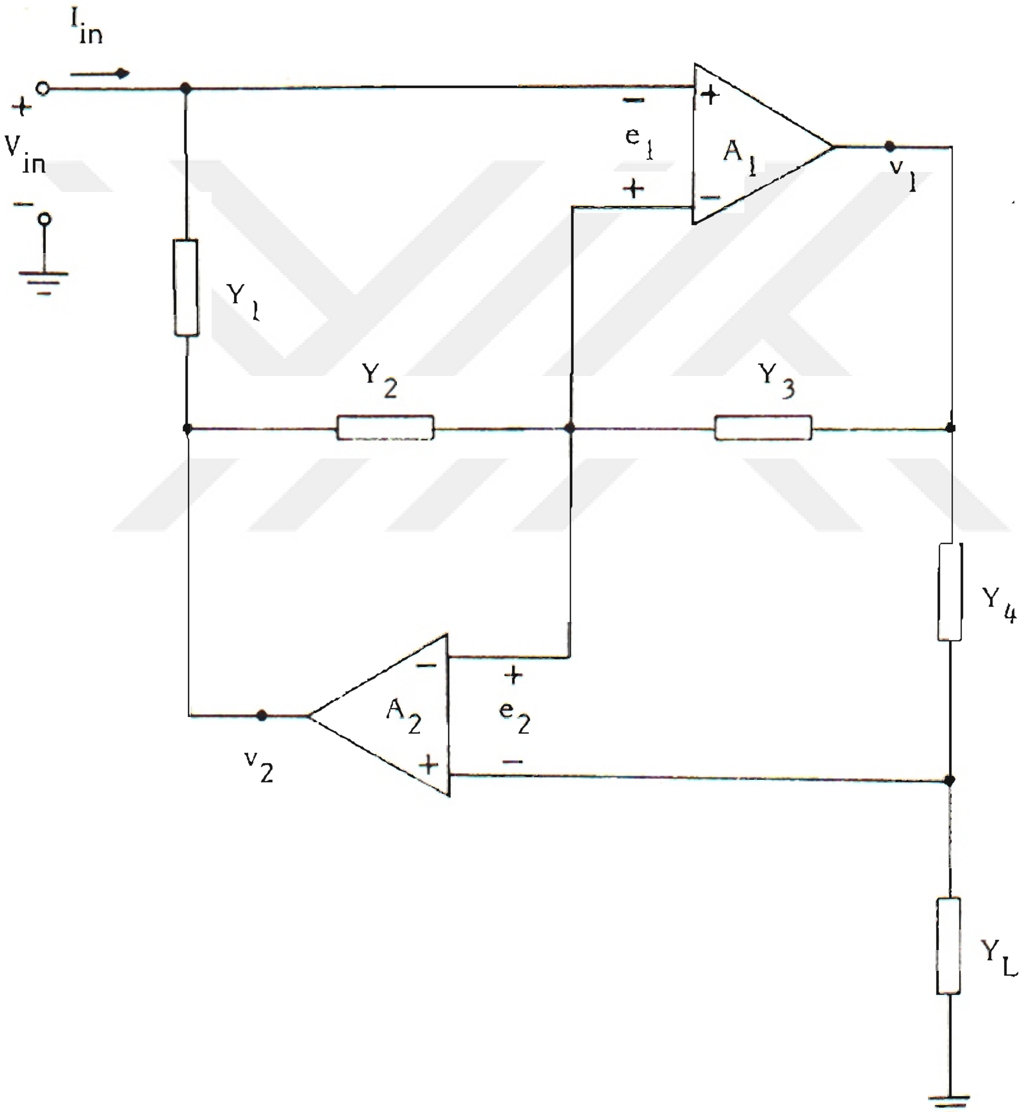

Figure 2.6.2 GIC Network

$$Z_{in_o}(s) = \frac{1}{Y_1} \frac{h_2 h_3}{h_1(1 - h_3)} = \frac{Y_2 Y_4}{Y_1 Y_3} \frac{1}{Y_L} = \frac{Z_1 Z_3}{Z_2 Z_4} Z_L$$

III. STABILITY

3.1 Introduction

In the time domain, a network is said to be stable if the output is bounded when a bounded input is applied. In the s-domain, the stability is determined by the location of the system poles. A network is stable if all of its poles are located in the open left half of the complex plane (LHP).

To determine the system poles, the transfer function of the network is expressed as the ratio of two polynomials. Then, the system poles are given by the roots of the polynominal in the denominator (the characteristic polynomical).

In this chapter, the characteristic determinant for n-OA networks is defined. Using this definition, first, the stability analysis for 1-OA networks is given. Then, the general case, n-OA stability problem, is stated using the eigenvalue theory. Also, some special cases are considered, in which the n-OA problem can be reduced to smaller sub-problems. Finally, the stability criterion at high frequencies is examined.

3.2 The Characteristic Determinant

In Section 2.3 the transfer function of an n-OA network is given as

$$T(s) = \frac{Q(s)}{P(s)} \tag{3.2.1}$$

where

$$Q(s) = \det \begin{bmatrix} A^{-1}+\beta & \gamma \\ \alpha & \zeta \end{bmatrix}$$

and

$$P(s) = \det \ (A^{-1} + \beta \ )$$

Definition 3.2.1: $P(s) = \det \ (A^{-1}+\beta \ )$ is called the characteristic determinant of an n-OA network.

The following theorem relates the stability of an n-OA network to its characteristic determinant.

Theorem 3.2.1: An n-OA network is stable if all the zeros of its characteristic determinant lie in the open LHP.

Proof: Q(s) and P(s) in equation 3.2.1 can be expressed as

$$Q(s) = \frac{N_1(s)}{D_1(s)}$$

$$P(s) = \frac{N_2(s)}{D_2(s)} \qquad (3.2.2)$$

where N_1, N_2, D_1, and D_2 are polynomials in s. Then, the transfer function expression becomes,

$$T(s) = \frac{N_1(s) \ D_2(s)}{D_1(s) \ N_2(s)} \qquad (3.2.3)$$

The poles of T(s) are given by the roots of $D_1(s)$ and $N_2(s)$. Since, the roots of $N_2(s)$ are the zeros of the characteristic determinant, to prove the theorem, it must be shown that $D_1(s)$ can have only stable roots.

The determinant of an nxn matrix is the sum of n! terms where each term is a product of n entries (only one entry is taken from each row and column) (ref. [28], p. 47). When terms are multiplied and added (or subtracted) as such, the denominator of the result is at most the least common denominator (LCD) of all the matrix entries. Because of the zero entries, some of the nonzero entries in the matrix may not appear in the determinant expression. In that case, the denominator of the result is a subset of the LCD of all the entries.

In view of the above discussion, the denominator of Q(s), $D_1(s)$, has the following property,

$$D_1(s) \subseteq \mathrm{LCD}\left(\frac{1}{A_i}, \beta_{ij}, \gamma_i, \alpha_j, \zeta\right) \qquad i=1,\ldots,n \quad j=1,\ldots,n$$

However, since β_{ij}, γ_i, α_j, and ζ are transfer functions obtained from a passive network, they have only stable poles. Also, the OAs have no zeros in the closed RHP, implying that $1/A_i$ does not have any poles in the closed RHP. Thus, $D_1(s)$ can have only stable roots. Therefore, the stability of an n-OA network is determined solely by the roots of $N_1(s)$, the numerator of the characteristic determinant.

The characteristic polynomial can be obtained from the characteristic determinant by expanding the latter. Using the two pole model of the OA (equation 2.2.1), the degree of the characteristic polynomial will be q=2n+k (n: the number of the OAs, k: the order of the passive feedback network). Thus, as the number of OAs is increased, the difficulty of determining the stability is also increased.

In the next section, the stability analysis of a 1-OA network is outlined to provide a basis for larger networks.

3.3 1-OA Stability

The characteristic determinant for 1-OA networks ($n = 1$) is

$$P(s) = A^{-1} + \beta \qquad (3.3.1)$$

To determine the location of the system poles, equation 3.3.1 is used. However, it is often time consuming to determine the roots of the resulting characteristic polynomial. Instead, the Nyquist criterion can be employed more efficiently.

When A is a monotonically decreasing function of frequency, then the Nyquist criterion reduces to the following simple test [8].

If $|\underline{/A} + \underline{/\beta}| < 180°$ when $|A| = 1/|\beta|$, then the network is stable, otherwise it is unstable.

The application of this test is fast and efficient in determining the stability of 1-OA networks. In the general case, however, A^{-1} and β are nxn matrices, and the characteristic determinant contains products of $1/A_i$'s and β_{ij}'s. Thus, this test can not be applied to n-OA networks.

In the next section, the n-OA problem will be factored into n 1-OA problems, by means of the eigenvalues of the characteristic determinant. Also, some special cases will be considered.

3.4 The Eigenvalue Problem

In the following theorem the stability of an n-OA network is described in terms of the eigenvalues of its characteristic matrix.

Theorem 3.4.1: Let $F(s) = A^{-1} + \beta$ be the characteristic matrix of an n-OA network and $\lambda_i(s)$, $i = 1,\ldots,n$ be the eigenvalues of $F(s)$. Then, the n-OA network is stable if none of the eigenvalues have zeros in the closed RHP.

Proof: From matrix theory (ref. [28] p. 283), it has been shown that the determinant of a matrix is the product of its eigenvalues,

$$\det [F(s)] = \prod_{i=1}^{n} \lambda_i(s) \qquad (3.4.1)$$

If none of the eigenvalues, $\lambda_i(s)$, have zeros in the closed RHP, neither will $\det[F(s)]$. Since $\det[F(s)]$ is the characteristic determinant of the network, using Theorem 3.2.1, the network will be stable.

This problem of finding the eigenvalues of F(s) can be simplified, if the OAs in the network are assumed to be identical.

Theorem 3.4.2: If for all the OAs in the network, the open-loop gains, A_i, are identical, then the eigenvalues of F(s), λ_i, can be written as

$$\lambda_i = \frac{1}{A_i} + \rho_i \qquad i = 1,\ldots,n \qquad (3.4.2)$$

where ρ_i are the eigenvalues of the β matrix.

Proof: If the open-loop gains of the OAs are identical, $A_1 = \ldots = A_n = A_i$, then, the matrix A^{-1} can be expressed as

$$A^{-1} = \mathrm{diag}\left(\frac{1}{A_1},\ldots,\frac{1}{A_n}\right) = \frac{1}{A_i}\, I \qquad (3.4.3)$$

where I is the identity matrix of order n. Then F(s) becomes

$$F(s) = \frac{1}{A_i}\, I + \beta \qquad (3.4.4)$$

The eigenvalues of F(s) are the roots of the following equation.

$$\det [\lambda I - F(s)] = 0 \qquad (3.4.5)$$

Substituting equation 3.4.4 into 3.4.5

$$\det \left[\left(\lambda - \frac{1}{A_i}\right) I - \beta\right] = 0 \qquad (3.4.6)$$

or setting $\lambda - \frac{1}{A_i} = \rho$

$$\det [\rho I - \beta] = 0 \qquad (3.4.7)$$

The roots of equation 3.4.7, ρ_i, are the eigenvalues of β. Thus, the eigenvalues of β and F(s) are related by

$$\rho_i = \lambda_i - \frac{1}{A_i}$$

or

$$\lambda_i = \frac{1}{A_i} + \rho_i$$

Thus, the theorem is proved.

These theorems simplify the n-OA stability problem to n 1-OA problems. However, the F(s) and β(s) matrices contain entries which are transfer functions in the s-domain. Hence, it is not a simple task to determine the eigenvalues, unless these matrices are of some special forms. These special forms are discussed below.

Corollary 3.4.1: If the β matrix is triangular (upper, lower, or diagonal), then the network is stable if and only if the terms

$$f_{ii}(s) = \left(\frac{1}{A_i} + \beta_{ii}\right) \qquad i = 1,\ldots,n \qquad (3.4.8)$$

have no zeros in the closed RHP.

Proof: When the β matrix is triangular, the F(s) matrix will also be triangular (since $F(s)=A^{-1}+\beta$ where A^{-1} is diagonal). But, the eigenvalues of a triangular matrix are its diagonal entries (ref. [29] p. 268). The diagonal entries of F(s), $f_{ii}(s)$, are given by equation (3.4.8). Thus, using Theorem 3.4.1, the network is stable if and only if none of the $f_{ii}(s)$ have zeros in the closed RHP.

A nonzero entry, β_{ij}, in the β matrix implies that there is a feedback connection from the jth OA output, v_j, to the ith OA input, e_i.

Thus, a diagonal β matrix is obtained when there is only one feedback path to each OA input which is from its own output. This is the trivial case of n non-interacting 1-OA networks. The lower (upper) triangular case occurs when the feedback connections to each OA input are made from its own output and the outputs of the preceeding (following) OAs (Figure 3.4.1).

Corollary 3.4.2: If the β matrix is block triangular (upper, lower, or diagonal) as shown below

$$\beta = \begin{bmatrix} B_{11} & \cdots & B_{1k} \\ & \ddots & \\ 0 & & B_{kk} \end{bmatrix} \quad \text{or} \quad \begin{bmatrix} B_{11} & & \\ \vdots & \ddots & 0 \\ B_{k1} & & B_{kk} \end{bmatrix} \quad \text{or} \quad \begin{bmatrix} B_{11} & & 0 \\ & \ddots & \\ 0 & & B_{Lk} \end{bmatrix}$$

where B_{jj}, $j=1,2,\ldots k$, are square matrices of order m_j, $(m_1+m_2+\ldots+m_k=n)$, then the network is stable if and only if the terms

$$Y_j(s) = \det\,[A_j^{-1} + B_{jj}] \qquad j = 1,\ldots,k \tag{3.4.9}$$

where A_j^{-1} is the jth principal minor of A^{-1} of size $m_j x m_j$, have no zeros in the closed RHP.

Proof: When the β matrix is block triangular, $F(s)=A^{-1}+\beta$ is also block triangular (since A^{-1} is a diagonal matrix). But, the eigenvalues of a block triangular matrix are the union of the eigenvalues of the diagonal blocks (submatrices) (ref. [29], p. 268). The diagonal blocks are given by $A_j^{-1}+B_{jj}$, which represent the characteristic matrices of sub-networks with m_j OAs. Thus, applying Theorem 3.4.1, the n-OA network is stable, when all of the sub-networks are stable, that is none of them have zeros in the closed RHP.

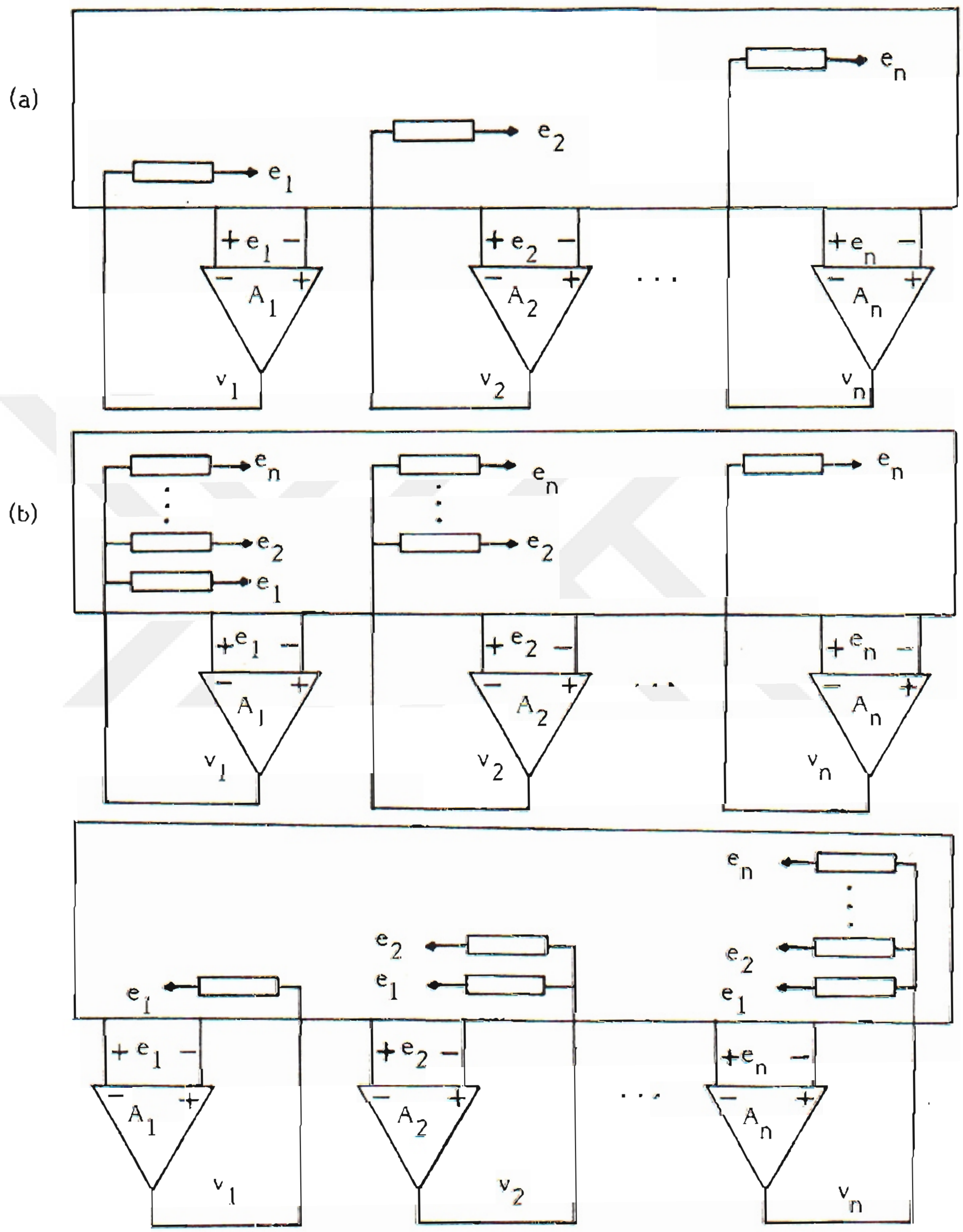

Figure 3.4.1 Feedback configurations resulting in (a) diagonal (b) lower triangular and (c) upper triangular β matrices

In this section, it has been shown that certain topologies of the feedback network result in sub-networks and the stability of the overall network depends on the stability of the individual sub-networks. In the next section another special case, diagonally dominant feedback networks, will be examined.

3.5 Diagonal Dominance

Definition 3.5.1 (ref. [29], p. 129): A matrix, $F(s)=[f_{ij}(s)]_{nxn}$, is diagonally dominant, if

$$|f_{ii}(s)| > \sum_{\substack{j=1 \\ j \neq i}}^{n} |f_{ij}(s)| \qquad (3.5.1)$$

or

$$|f_{ii}(s)| > \sum_{\substack{j=1 \\ j \neq i}}^{n} |f_{ji}(s)| \qquad (3.5.2)$$

where $|\cdot|$ denotes the magnitude when $s = j\omega$.

Stability criterion for such matrices is stated in the following theorem.

Theorem 3.5.1: Assume a network is represented by a characteristic matrix, F(s), which is diagonally dominant. If the diagonal entries of F(s) have no zeros in the closed RHP, then neither do the eigenvalues of F(s), and the network is stable.

Proof: Two well-known theorems, stated below, are needed for this proof.

Gershgorin's Theorem (ref. [29], p. 302): Given an nxn matrix,

$F(s)=[f_{ij}]$, all of its eigenvalues are contained in the union of n discs whose centers, c_i, and radii, r_i, are given by

$$c_i = f_{ii} \quad \text{and} \quad r_i = \sum_{\substack{j=1 \\ j \neq i}}^{n} |f_{ij}| \qquad (3.5.3)$$

or

$$c_i = f_{ii} \quad \text{and} \quad r_i = \sum_{\substack{j=1 \\ j \neq i}}^{n} |f_{ji}| \qquad (3.5.4)$$

Rouche's Theorem (ref. [30] p. 285): If g(s) and h(s) are each functions which are analytic inside and on a simple closed contour, D, and if the strict inequality

$$|h(s) - g(s)| < g(s)$$

holds at each point on D, then g(s) and h(s) must have the same number of zeros (counting multiplicity) inside D.

Now, if the eigenvalues of F(s) are denoted by $\lambda_i(s)$, then according to the Gershgorin's Theorem, $\lambda_i(s)$ are contained in the union of the discs whose equations are given by

$$|\lambda_i(s) - f_{ii}(s)| \leq r_i \qquad i = 1,\ldots,n \qquad (3.5.5)$$

But the diagonal dominance suggests that

$$r_i < |f_{ii}(s)| \qquad (3.5.6)$$

Thus, equation 3.5.5 can be expressed as

$$|\lambda_i(s) - f_{ii}(s)| < |f_{ii}(s)| \qquad (3.5.7)$$

Now, applying Rouche's Theorem to equation 3.5.7 (contour D being the semicircle which encloses the entire closed RHP), it can be stated that $\lambda_i(s)$ and $f_{ii}(s)$ must have the same number of zeros in the closed RHP. Thus, if the diagonal entries, $f_{ii}(s)$, have no zeros in the unstable region, neither will the eigenvalues. Then, by Theorem 3.4.1, the network will be stable.

The conditions for stability, as outlined by Theorem 3.5.1, are sufficient but not necessary. That is, if a network does not satisfy the requirements of this theorem, then no statement can be made about its stability. In the next section, another stability theorem is developed which is necessary but not sufficient.

3.6 High frequency Stability

In an n-OA network two types of system poles exist:

(a) Ideal poles: These are the poles when the OAs are assumed ideal ($GB = \infty$). The ideal poles of a network are also called the design poles or the desired poles.

(b) Parasitic poles: These are the poles due to the finite GB OAs. If the two-pole model of the OA is employed, then each OA in the network contributes two parasitic poles to the system.

The presence of the parasitic poles tends to move the ideal poles towards the RHP, thus making the stability conditions worse (ref. [31], p. 426). The sensitivity of the poles due to the finite GB is studied in the next chapter. In addition to the movement of the ideal poles, a network can become unstable due to the parasitic poles located in the RHP. If the network is designed at low frequencies, i.e. the design frequency, ω_o, is much smaller than the GBs of the OAs, $(\frac{\omega_o}{GB} << 1)$, then the ideal pole movement is negligible and the parasitic poles determine the stability. As the design frequency is increased (or equivalently GB is decreased) the parasitic poles move toward the origin in a constant Q manner [15]. Thus, if a network is unstable for the low frequency design, then it will be unstable when the design frequency is increased.

For a low frequency design, the capacitors behave like short circuits at frequencies close to the GBs of the OAs. Then, the passive feedback network looks like a resistive circuit, yielding a β matrix whose entries are resistor ratios. Thus, the stability at high frequencies is determined by the eigenvalues of

$$F'(s) = A^{-1} + \beta_C \qquad (3.6.1)$$

where

$$\beta_C = \lim_{s \to \infty} \beta(s)$$

If all the OAs in the network are assumed identical, then the eigenvalues of $F'(s)$, λ'_i, are given by

$$\lambda'_i = \frac{1}{A_i} + \rho'_i \qquad i = 1,\ldots,n \qquad (3.6.2)$$

where ρ'_i, represent the eigenvalues of β_C. Since β_C is a constant matrix, the eigenvalue problem is much easier compared to the case of Theorem 3.4.2. Once the eigenvalues are determined, the 1-OA stability test can be applied to equation 3.6.2. If the network passes the high frequency stability (HFS) test, then the parasitic poles are in the LHP. However, the network may still be unstable due to the ideal pole movements. So, for a network to be stable, it is necessary but not sufficient to satisfy the HFS criterion.

It is important to note that, when the feedback network is resistive (Active-R networks), the HFS criterion is both necessary and sufficient, since the only poles of such networks are the parasitic poles. The β matrix describing the feedback is already a constant matrix.

IV. ACTIVE SENSITIVITY

4.1 Introduction

In designing a network, the transfer function is the first requirement to be met. In the literature, many equivalent configurations realizing the same ideal transfer function can be found. The criterion for selecting one of these configurations is the performance of the network (along with the basic criteria, such as cost, availability, and flexibility). Sensitivity is an important measure of performance.

The original design can change drastically due to changes in the network (component tolerances, aging, capacitor losses, etc.) and in the environment (temperature, humidity, etc.). The methods to determine the sensitivity of a design due to these changes are well established. However with the introduction of active components such as OAs into the network design another type of sensitivity , active sensitivity, has become a significant design factor. Active sensitivity can be defined as the deviations from the original design caused by the nonideal behavior of the active components in the network. In our case, the active component is the OA and the non-ideal behavior is the finite GB.

The transfer function of a network is characterized by its poles and zeros. Any changes in the locations of the poles and zeros directly effect the frequency response of the network. In this chapter, the active sensitivity expressions for the poles and zeros are derived.

4.2 OA Variations

Initial design of an n-OA network is achieved by assuming ideal OAs, that is the open-loop gain of each OA, A_i, is assumed to be infinite. However, the actual A_i, as described by equation 2.2.1, is not only finite but also frequency dependent. If it is assumed that the GB is the only varying parameter of the open-loop gain, then any change in the GB varies A and as a result the ideal poles and zeros are perturbed from their designed locations. In order to determine the sensitivity of the ideal poles and zeros with respect to the GBs of the OAs, it is necessary to derive the variation in A with respect to the GB.

Since the reciprocal of A appears in the transfer function expression, a new variable, U, is defined below.

$$U_i = \frac{1}{A_i} = \tau_i \, (\theta_i \tau_i s + 1)(s + \omega_{L_i}) \qquad (4.2.1)$$

where $\tau_i = 1/GB_i$ and $\theta_i = 1/k_i$. Thus, for an ideal OA, τ_i and U_i are zero. In determining the sensitivity expressions U_i and τ_i will be used in place of A_i and GB_i for convenience.

Any variation in τ_i causes a change in U_i, which can be determined by differentiating equation 4.2.1 with respect to τ_i. This change evaluated at the ideal value of τ_i is given by

$$\left.\frac{\partial U_i}{\partial \tau_i}\right|_{\tau_i = 0} = (s + \omega_{L_i}) \qquad (4.2.2)$$

Here, it is assumed that the OAs are statistically independent of each other, i.e. τ_j does not effect U_i when $j \neq i$.

4.3 Sensitivity of the Ideal Poles

The transfer function of an n-OA network is given by Theorem 2.3.1,

$$T(s) = \frac{\det \begin{bmatrix} U+\beta & \gamma \\ \alpha & \zeta \end{bmatrix}}{\det (U + \beta)} \tag{4.3.1}$$

and the ideal gain expression is given by Corollary 2.3.1

$$K(s) = \frac{B'(s)}{B(s)} = \frac{\det \begin{bmatrix} \beta & \gamma \\ \alpha & \zeta \end{bmatrix}}{\det (\beta)} \tag{4.3.2}$$

The ideal poles of the network, $p_{o1} \ldots p_{ok}$, are found by setting $B(s) = 0$. The changes in the ideal poles due to τ_i can be best observed by the Maclauin series expansion [7]. For small changes, the series can be approximated by the first order terms as given below.

$$p_j(\tau_1, \ldots, \tau_n) = p_{jo} + \sum_{i=1}^{n} \left. \frac{\partial s}{\partial \tau_i} \right|_{\substack{\tau_1 = \ldots = \tau_n = 0 \\ s = p_{jo}}} \cdot \tau_i \tag{4.3.3}$$

The derivative terms in equation 4.3.3 can be derived by differentiating the denominator of $T(s)$ which determines the actual poles.

$$\frac{\partial}{\partial \tau_i} [\det (U + \beta)] = 0 \qquad i = 1, \ldots, n \tag{4.3.4}$$

The derivative of the determinant of an nxn matrix is the sum of n nxn determinants, where the jth determinant is obtained by differentiating the jth row of the original matrix (ref. [28], p. 72). Using this rule and equation 4.2.2, it can be shown that

$$(s + \omega_{L_i}) B_{ii}(s) + \frac{\partial B(s)}{\partial \tau_i} = 0 \tag{4.3.5}$$

when $\tau_1 = \ldots = \tau_n = 0$. $B_{ii}(s)$ denotes the determinant of β when row i and column i are deleted.

The denominator of the ideal transfer function, B(s), can be expressed as

$$B(s) = C_B \frac{\prod_{i=1}^{k} (s - p_{io})}{D_B(s)} \tag{4.3.6}$$

where C_B is a constant, $D_B(s)$ is a polynomial in s, and p_{io}, i=1,...,k are the ideal poles of the network. Then,

$$\left.\frac{\partial B(s)}{\partial s}\right|_{s = p_{jo}} = \frac{C_B}{D(p_{jo})} \prod_{\substack{i=1 \\ i \neq j}}^{k} (p_{jo} - p_{io}) \tag{4.3.7}$$

(Note that when k=1, the product term in the above expression becomes 1). Using the chain rule, the derivative term in equation 4.3.5 can be expressed as,

$$\frac{\partial B(s)}{\partial \tau_i} = \frac{\partial B(s)}{\partial s} \frac{\partial s}{\partial \tau_i} \tag{4.3.8}$$

Now, the derivative terms in the Maclaurin series expansion can be derived using equations 4.3.5, 4.3.7, and 4.3.8

$$\left.\frac{\partial s}{\partial \tau_i}\right|_{\substack{s = p_{jo} \\ \tau_1 = \dots = \tau_n = 0}} = -D_B(p_{jo}) \frac{\sum_{i=1}^{n} (p_{jo} + \omega_{L_i}) B_{ii}(p_{jo}) \cdot \tau_i}{C_B \prod_{\substack{i=1 \\ i \neq j}}^{k} (p_{jo} - p_{i0})} \qquad (4.3.9)$$

Inserting equation 4.3.9 into equation 4.3.3, the change in the jth pole can be written as

$$\Delta p_j = p_j - p_{jo} = -D_B(p_{jo}) \frac{\sum_{i=1}^{n} (p_{jo} + \omega_{L_i}) B_{ii}(p_{jo}) \tau_i}{C_B \prod_{\substack{i=1 \\ i \neq j}}^{k} (p_{jo} - p_{io})} \qquad (4.3.10)$$

This expression can be simplified, if the OAs are assumed to be matched, i.e. $\omega_{L_1} = \dots = \omega_{L_n} = \omega_L$ and $\tau_1 = \dots = \tau_n = \tau = 1/GB$. In this case equation 4.3.10 is reduced to the following.

$$\Delta p_j = -\frac{p_{jo} + \omega_L}{GB} \frac{D_B(p_{jo}) \sum_{i=1}^{n} B_{ii}(p_{jo})}{C_B \prod_{\substack{i=1 \\ i \neq j}}^{k} (p_{jo} - p_{i0})} \qquad (4.3.11)$$

Since $B_{ii}(s)$ are the determinants derived from the β matrix, when added together, the denominator of the sum will be $D_B(s)$ and the numerator will be a polynomial in s of order $\ell \leq k$.

$$\sum_{i=1}^{n} B_{ii}(s) = \frac{C_p}{D(s)} \prod_{i=1}^{\ell} (s - s_{ip}) \qquad (4.3.12)$$

where C_p is the coefficient of s^{ℓ} and s_{ip} are the roots of the numerator. Substituting equation 4.3.12 into equation 4.3.11,

$$\Delta p_j = -\frac{C_p}{C_B} \frac{p_{jo} + \omega_L}{GB} \frac{\prod_{i=1}^{\ell} (p_{jo} - s_{ip})}{\prod_{\substack{i=1 \\ i \neq j}}^{k} (p_{jo} - p_{io})} \qquad (4.3.13)$$

The ideal poles, $p_{1o} \ldots p_{ko}$, are fixed by the design requirement; ω_L and GB are the parameters of the OAs in the network. In order to minimize the pole sensitivities given by equation 4.3.13, independent of the OAs and ideal design, s_{ip} must be very close to p_{jo} and/or the ratio C_p/C_B must be made as small as possible.

4.4 Sensitivity of the Ideal Zeros

Expressions similar to equation 4.3.10 and 4.3.13 can be derived for the sensitivity of the ideal zeros, this time using the numerator of the transfer function.

Similar to equation 4.3.6, the ideal numerator, B', can be expressed as the ratio of two polynomials,

$$B'(s) = C_B' \frac{\prod_{i=1}^{k'} (s - z_{io})}{D_B(s)} \qquad (4.4.1)$$

where $k' \leq k$, C_B' is the coefficient of the highest order term in the numerator, and z_{io} are the roots of the numerator, which are the ideal zeros of the network. The denominators of B(s) and $B'(s)$ are given by the same polynomial, $D_B(s)$.

Following the same steps taken in the preceeding section, the expression for the change in the zeros of the ideal transfer function due to τ_i, is derived.

$$z_j = z_j - z_{jo} = - D_B(z_{jo}) \frac{\sum_{i=1}^{n} (z_{jo} + \omega_{L_i}) B'_{ii}(z_{jo}) \tau_i}{C'_B \prod_{\substack{i=1 \\ i \neq j}}^{k} (z_{jo} - z_{io})} \qquad (4.4.2)$$

where $B'_{ii}(s)$ is obtained from $B'(s)$ by deleting row i and column i. The product term in the denominator is equal to unity when $k' = 1$.

In the case of identical OAs, the terms containing identical OA parameters can be factored out of the summation term in equation 4.4.2 and the remainder can be expressed as

$$\sum_{i=1}^{n} B'_{ii}(s) = C_z \frac{\prod_{i=1}^{\ell'} (s - s_{iz})}{D_B(s)} \qquad (4.4.3)$$

where $\ell' \leq k$, C_z is the coefficient of the highest order term in the numerator, and s_{iz} are the roots of the numerator. Thus, equation 4.4.2 becomes

$$\Delta z_j = - \frac{C_z}{C'_B} \frac{z_{jo} + \omega_L}{GB} \frac{\prod_{i=1}^{\ell'} (z_{jo} - s_{iz})}{\prod_{\substack{i=1 \\ i \neq j}}^{k} (z_{jo} - z_{io})} \qquad (4.4.4)$$

4.5 Graphical Interpretation

In the pole sensitivity expression of equation 4.3.12, each term can be viewed as vectors in the complex plane. Then, the pole sensitivity expression can be rewritten as,

$$\Delta p_j = C_{qi} \frac{\prod_{i=1}^{\ell} q_{ji}}{\prod_{\substack{i=1\\ i\neq j}}^{k} q_{jio}} \qquad (4.5.1)$$

where

$$C = -\frac{C}{C_B}\frac{1}{GB}$$

$q_{jL} = (p_{jo} - (-\omega_L))$; the vector drawn from $-\omega_L$ to p_{jo},

$q_{ji} = (p_{jo} - s_{ip})$; the vector drawn from s_{ip} to p_{jo}, and

$q_{jio} = (p_{jo} - p_{io})$; the vector drawn from p_{io} to p_{jo}.

In terms of the magnitude and angles of these vectors, the magnitude and the angle of the pole sensitivity are given by

$$|\Delta p_j| = |C||q_{jL}| \frac{\prod_{i=1}^{\ell} |q_{ji}|}{\prod_{\substack{i=1\\ i\neq j}}^{k} |q_{jio}|}$$

and

$$\underline{/\Delta p_j} = \pm 180° + \underline{/q_{iL}} + \sum_{i=1}^{\ell} \underline{/q_{ij}} - \sum_{\substack{i=1\\ i\neq j}}^{k} \underline{/q_{jio}}$$

For an arbitrary network with a pair of complex conjugate ideal poles ($k=\ell=2$), the vectors for Δp_1, and Δp_2 are shown in Figure 4.5.1 and Figure 4.5.2 respectively. Observing these two figures and magnitude and phase expressions, Δp_1 is related to Δp_2 by

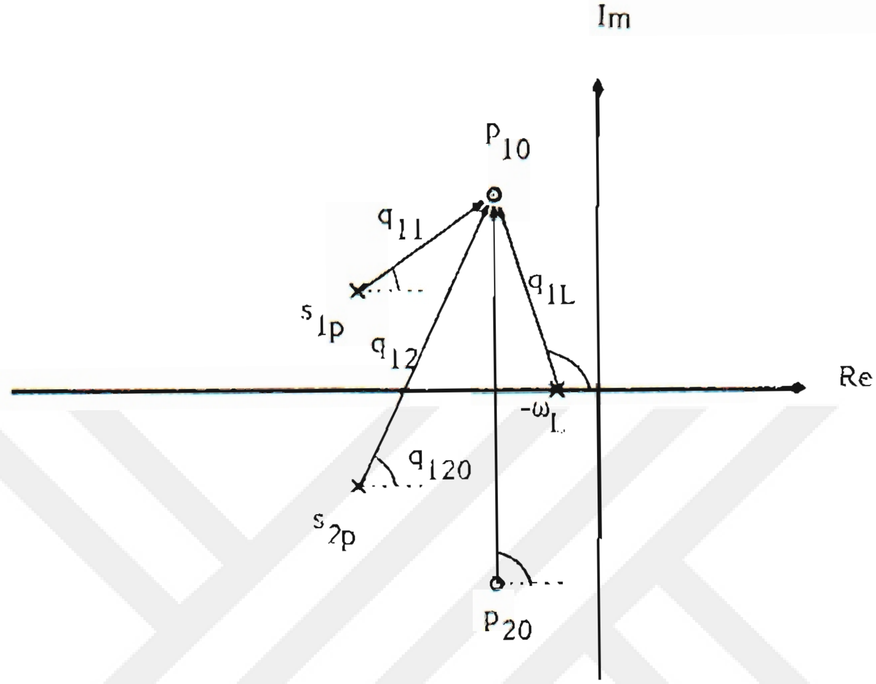

Figure 4.5.1 Sensitivity diagram for p_{10}

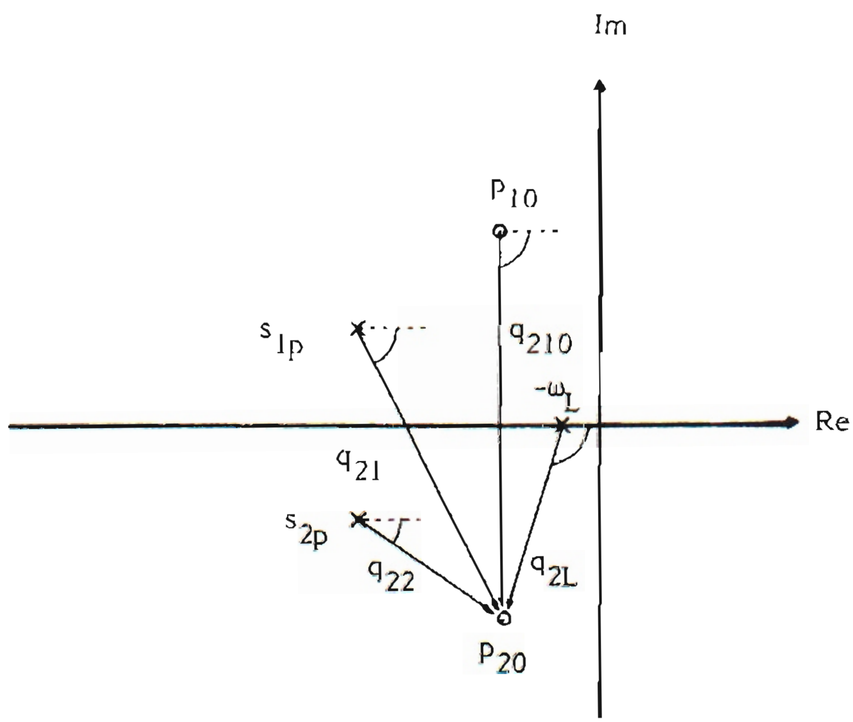

Figure 4.5.2 Sensitivity diagram for p_{20}

$$|\Delta p_1| = |\Delta p_2|$$

and

$$\underline{/\Delta p_1} = - \underline{/\Delta p_2}$$

Thus, it can be deduced that, for a pair of complex conjugate ideal poles, the corresponding pole sensitivites will also be a complex conjugate pair.

The pole sensitivities can also be used to determine the ideal pole movements. If the real part of Δp_1 or Δp_2 is positive, then the ideal poles will move towards the RHP. The real part of the pole sensitivities is positive when Δp_1 and Δp_2 are in the first or fourth quadrant, (i.e. $-90° < ang(\Delta p) < 90°$).

V. NETWORK GENERATION

5.1 Introduction

From an n-OA network, it is possible to generate new networks with the same ideal characteristics. This is accomplished by modifying the OA connections while keeping the feedback network unchanged. In this chapter, the theory of network generation by means of relocating the OAs is presented. In addition, a technique for improving the stability is outlined.

5.2 OA Relocation

The OA is a three terminal device; e^+ and e^- are the input terminals and v is the output terminal. In an n-OA network, the OAs are connected to the feedback network by way of these terminals. Depending on where these connections are made, the network is described by a set of equations defined by β, γ, α, and ζ. If the OA connections are changed, a new network is obtained which is described by a new set of matrices β_r, γ_r, α_r, and ζ_r. OA relocation is a method of reconnecting the OAs in such a way that the new set of system matrices yields the original ideal gain. There are two types of OA relocation: (a) Output relocation, (b) Input relocation. In the former the output terminals and in the latter the input terminals of the OAs are relocated.

5.2.1 Output Relocation

Theorem 5.2.1: Given an n-OA network as shown in Figure 5.2.1 (a),

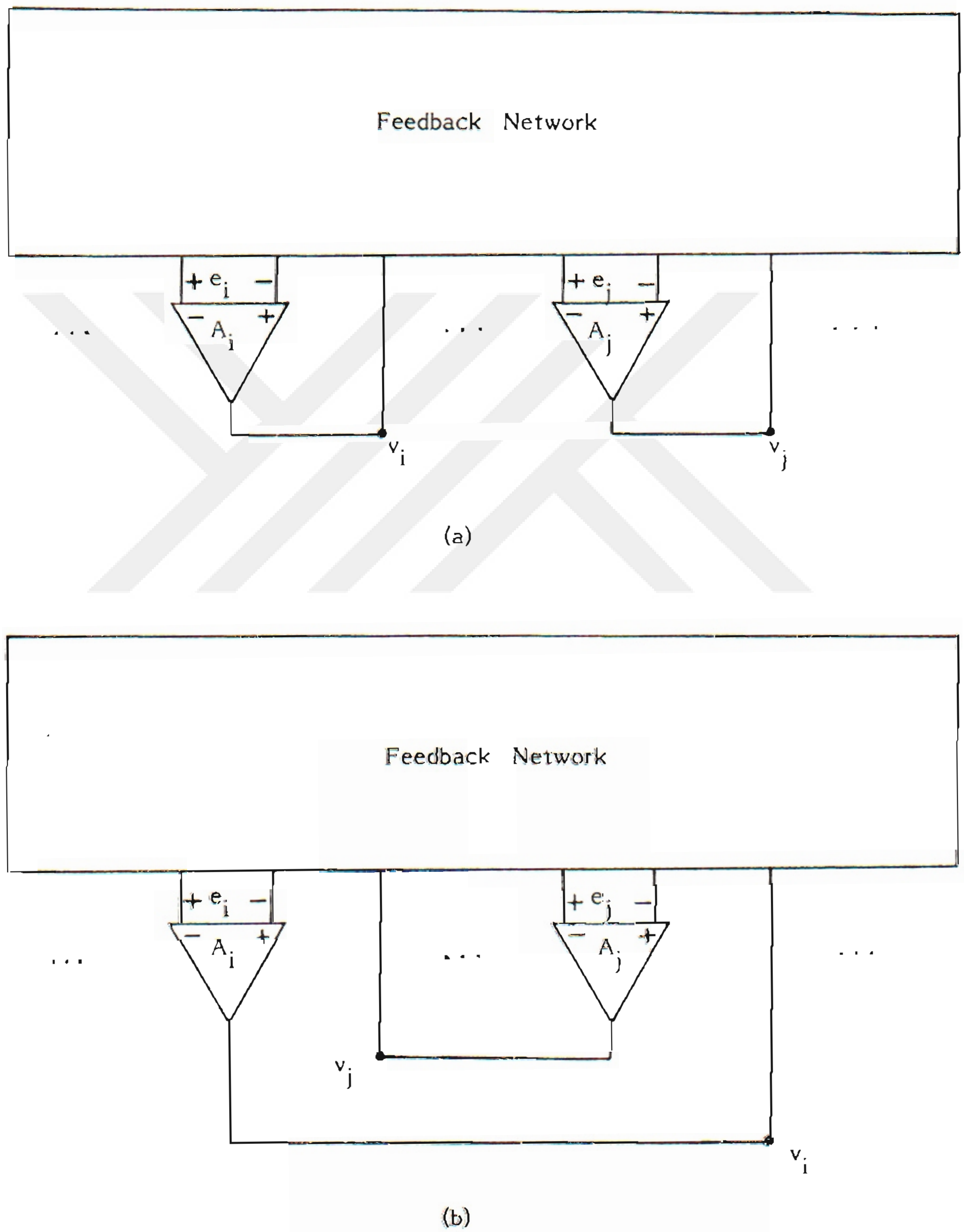

Figure 5.2.1 Output relocation, (a) original network, (b) relocated network

if the outputs of the ith and jth OAs, v_i and v_j, are interchanged (Figure 5.2.1 (b)), then the ith and jth columns of β and α are also interchanged and the ideal gain remains unchanged.

Proof: For the original network (Figure 5.2.1 (a)), the system equations are

$$\begin{bmatrix} e_1 \\ \cdot \\ \cdot \\ \cdot \\ e_n \\ V_o \end{bmatrix} = \begin{bmatrix} \cdots & \beta_{1i} & \cdots & \beta_{ij} & \cdots \\ & \cdot & & \cdot & \\ & \cdot & & \cdot & \\ & \cdot & & \cdot & \\ \cdots & \beta_{ni} & \cdots & \beta_{nj} & \cdots \\ \cdots & \alpha_i & \cdots & \alpha_j & \cdots \end{bmatrix} \begin{bmatrix} \vdots \\ v_i \\ \vdots \\ v_j \\ \vdots \\ V_{in} \end{bmatrix}$$

When v_i and v_j are interchanged as shown in Figure 5.2.1 (b), then the system equations for the resulting network can be written as,

$$\begin{bmatrix} e_i \\ \cdot \\ \cdot \\ \cdot \\ e_n \\ V_o \end{bmatrix} = \begin{bmatrix} \cdots & \beta_{ii} & \cdots & \beta_{ij} & \cdots \\ & \cdot & & \cdot & \\ & \cdot & & \cdot & \\ & \cdot & & \cdot & \\ \cdots & \beta_{ni} & \cdots & \beta_{nj} & \cdots \\ \cdots & \alpha_i & \cdots & \alpha_j & \cdots \end{bmatrix} \begin{bmatrix} \vdots \\ v_j \\ \vdots \\ v_i \\ \vdots \\ V_{in} \end{bmatrix}$$

Equation 5.2.2 can be rewritten, restoring the original locations of v_i and v_j,

$$\begin{bmatrix} e_i \\ \cdot \\ \cdot \\ \cdot \\ e_n \\ V_o \end{bmatrix} = \begin{bmatrix} \cdots & \beta_{ij} & \cdots & \beta_{ii} & \cdots \\ & \cdot & & \cdot & \\ & \cdot & & \cdot & \\ & \cdot & & \cdot & \\ \cdots & \beta_{nj} & \cdots & \beta_{ni} & \cdots \\ \cdots & \alpha_j & \cdots & \alpha_i & \cdots \end{bmatrix} \begin{bmatrix} \vdots \\ v_i \\ \vdots \\ v_j \\ \vdots \\ V_{in} \end{bmatrix}$$

Comparing equations 5.2.1 and 5.2.3, it is seen that the generated network has the same system matrices as the original, except the ith and jth columns of β and α are interchanged.

The ideal gain of the generated network, $K_r(s)$, is given by

$$K_r(s) = \frac{B_r'}{B_r}$$

where

$$B_r = \det(\beta_r)$$

and

$$B_r' = \det \begin{bmatrix} \beta_r & \gamma \\ \alpha_r & \zeta \end{bmatrix}$$

Since β_r and α_r are obtained from β and α by interchanging two rows, then $B_r = -B$ and $B_r' = -B'$ (ref. [32] p. 255). Thus,

$$K_r(s) = \frac{-B'}{-B} = \frac{B'}{B} = K(s)$$

therefore, the ideal gain of the generated network is the same as the ideal gain of the original network.

5.2.2 Input Relocation

Input relocation is subdivided into three catagories, (i) Sign change, (ii) Port relocation, and (iii) Node relocation. These three types of input relocation are described in the following theorems.

Theorem 5.2.2: Given an n-OA network, if the input terminals of the ith OA are reversed, (Figure 5.2.2), then the ith rows of β and γ are multiplied by -1 and the ideal gain remains unchanged.

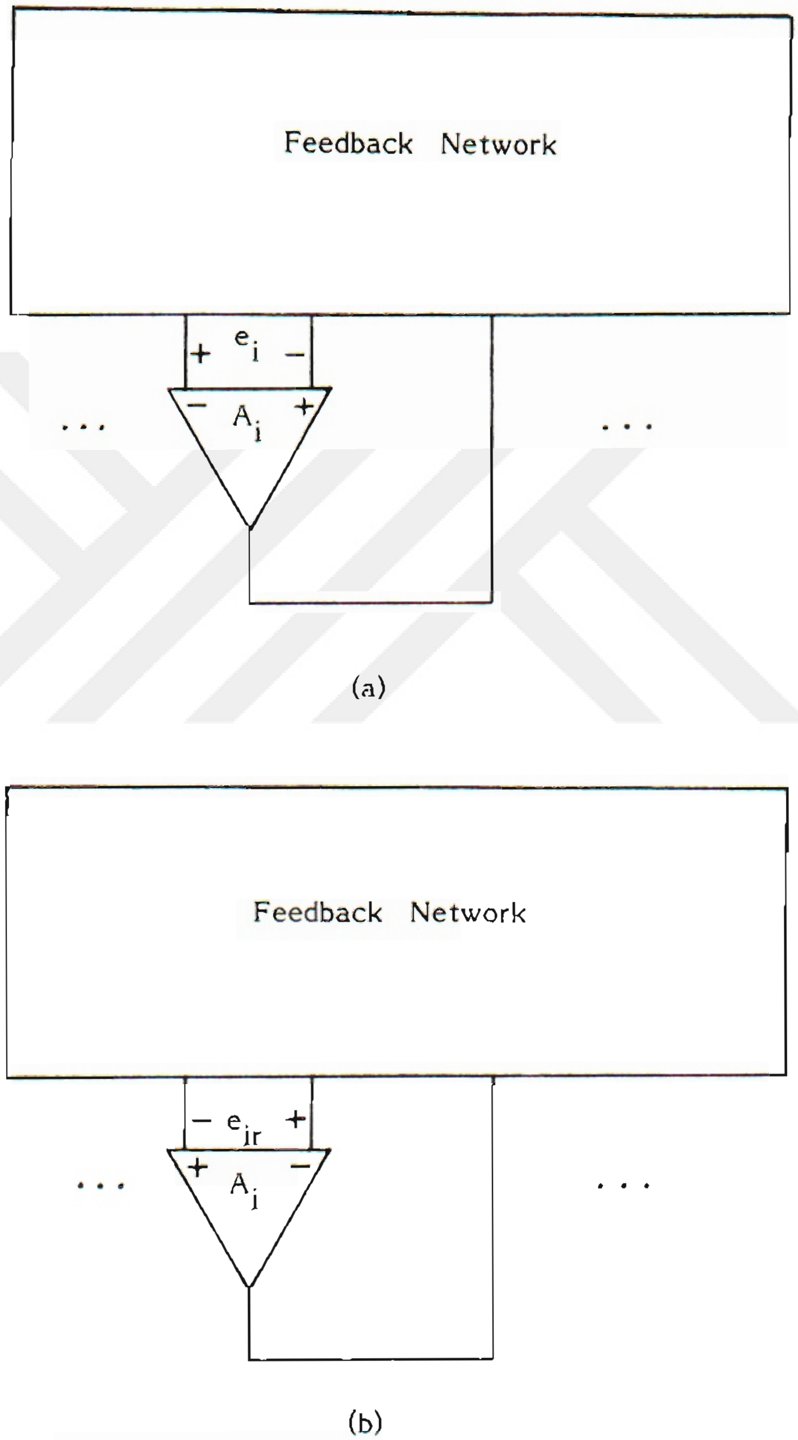

Figure 5.2.2 Input (sign change) relocation
(a) original network, (b) relocated network

Proof: For the original network of Figure 5.2.2 (a), e_i is given by

$$e_i = \beta_{i1} v_1 + \ldots + \beta_{in} v_n + \gamma_i v_{in}$$

but for the relocated network of Figure 5.2.2 (b)

$$e_{ir} = -e_i = -(\beta_{i1} v_1 + \ldots + \beta_{in} v_n + \gamma_i V_{in})$$

Thus, the generated network will have the same system matrices except the ith rows of β and γ are multiplied by -1. When a row or column of a matrix is multiplied by a constant, then the determinant of that matrix is also multiplied by the same constant (ref. [32], p. 257). Therefore, $B_r = -B$ and $B_r' = -B'$, and the ideal gain of the generated network is

$$K_r(s) = \frac{B_r'}{B_r} = \frac{-B'}{-B} = \frac{B'}{B}$$

which is the same as the ideal gain of the original network.

Theorem 5.2.3: In an n-OA network, if the input ports (e^+-e^- pair) of the ith and jth OAs are interchanged (Figure 5.2.3), then the ith and jth rows of β and γ are also interchanged and the ideal gain is not affected.

Proof: For the original network (Figure 5.2.3 (a)), the following equations are written.

$$e_i = \beta_{i1} v_1 + \ldots + \beta_{in} v_n + \gamma_i V_{in}$$

and

$$e_j = \beta_{j1} v_1 + \ldots + \beta_{jn} v_n + \gamma_j V_{in}$$

when the two input ports are interchanged as shown in Figure 5.2.3 (b), then

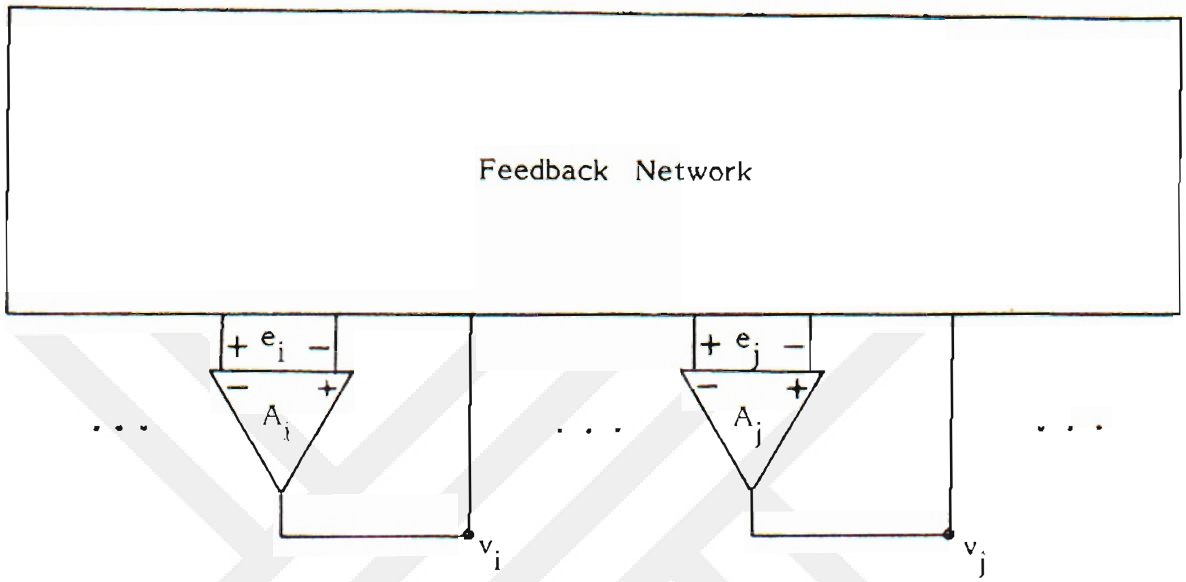

(a)

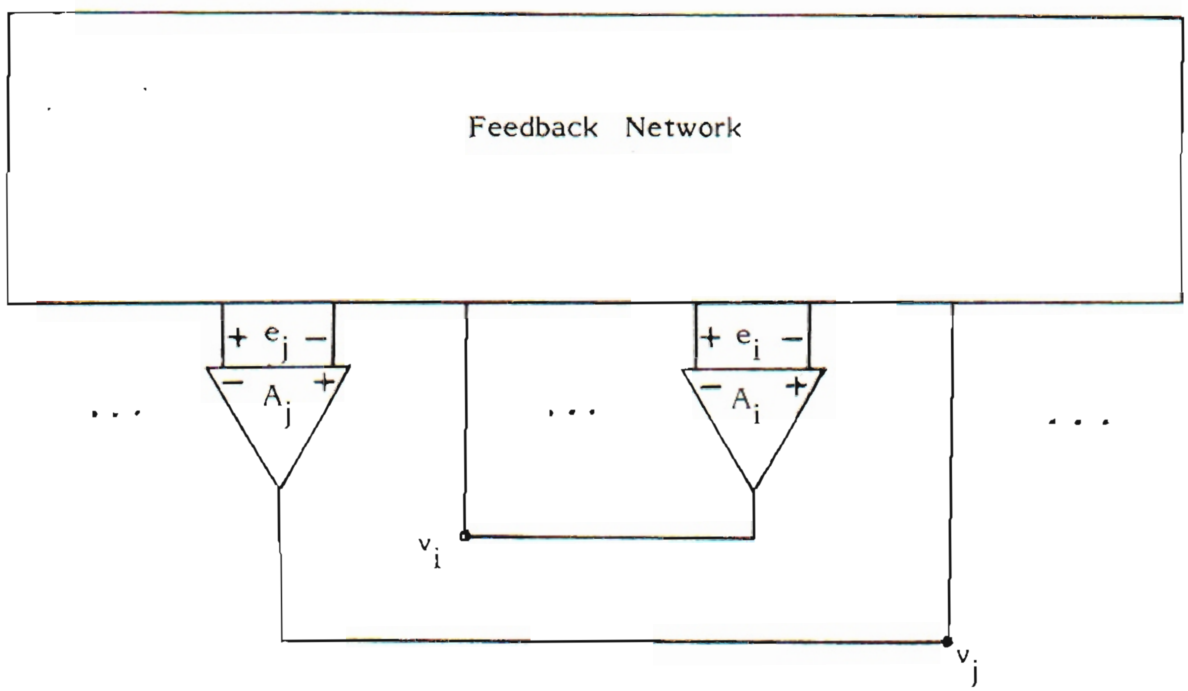

(b)

Figure 5.2.3 Input (port) relocation, (a) original network, (b) relocated network

$$e_{ir} = e_j = \beta_{j1} v_1 + \ldots + \beta_{jn} v_n + \gamma_j V_{in}$$

and

$$e_{jr} = e_i = \beta_{i1} v_1 + \ldots + \beta_{in} v_n + \gamma_i V_{in}$$

Thus, the system matrices of the generated network can be obtained from the original matrices by interchanging the ith and jth rows of β and γ. Since, interchanging two rows of a matrix negates its determinant, then, as before,

$$K_r(s) = \frac{B_r'}{B_r} \quad \frac{-B'}{-B} \quad \frac{B'}{B}$$

Therefore, the ideal gain is not affected.

<u>Remark 5.2.1:</u> If the input port and output relocations (Theorems 5.2.1 and 5.2.2) are applied simultaneously to the ith and jth OAs, the result is the same as interchanging the ith and jth OAs (Figure 5.2.4). Thus, if A_i and A_j are identical, then the generated network is not a new one.

<u>Proof:</u> The proof follows from Figure 5.2.4.

<u>Theorem 5.2.4:</u> Assume an n-OA network is given in which the input terminals of two OAs are connected at a common node as shown in Figure 5.2.5 (a). If $e_i^{\mp}$ $[e_j^{\pm}]$ is moved from the common node to $e_j^{\mp}$ $[e_i^{\pm}]$ as shown in Figure 5.2.5 (b), then β_r and γ_r of the resulting network are obtained by replacing the ith [jth] rows of β and γ with

i) (row(i)-row(j)) [row(j)-row(i)], if, in the original network, the connected input nodes are of identical signs,

ii) (row(i)+row(j)) [row(j)+row(i)], if, in the original network, the connected input nodes are of opposite signs.

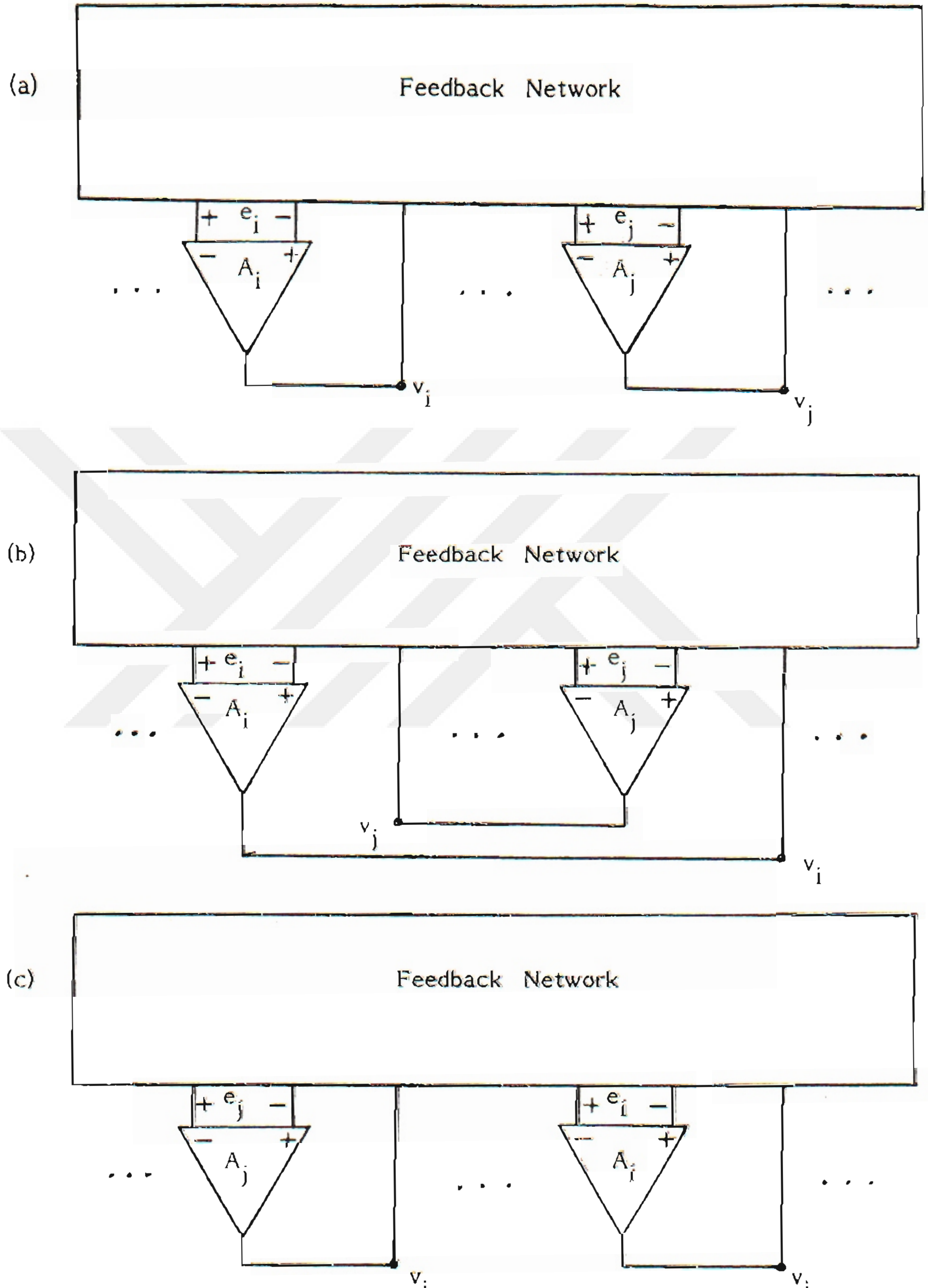

Figure 5.2.4 Illustration of Remark 5.2.1, (a) original network, (b) output relocation, (c) input port relocation

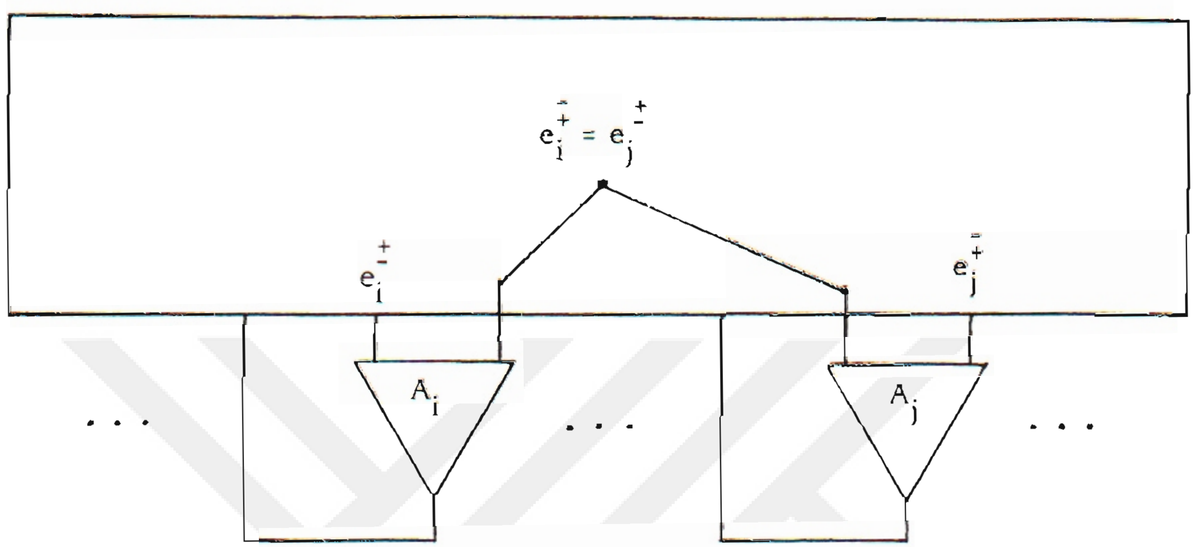

(a)

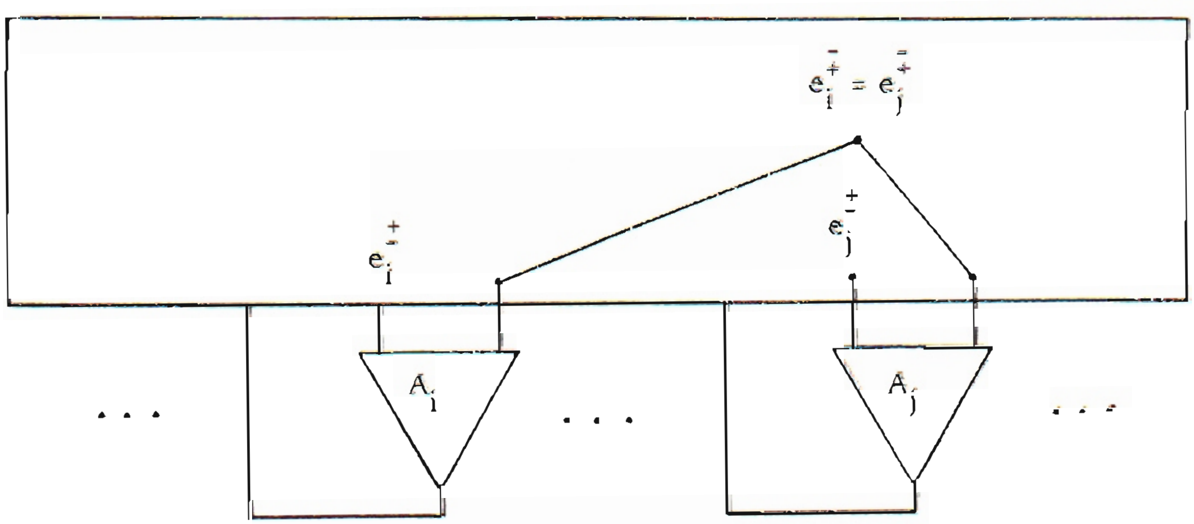

(b)

Figure 5.2.5 Input (node) relocation, (a) original network (b) relocated network

In either case, the ideal gain remains unaffected.

Proof: There are four possible ways the two input nodes may be connected at the common node: (i) $e_i^- = e_j^-$, (ii) $e_i^+ = e_j^+$, (iii) $e_i^- = e_j^+$, and (iv) $e_i^+ = e_j^-$. Since, the proofs of these four cases are similar, only the first will be provided.

i) Assume that, in the original network, e_i^- and e_j^- are connected, then, the following equations can be written.

$$e_i = e_i^+ - e_i^- \tag{5.2.4}$$

$$e_j = e_j^+ - e_j^- \tag{5.2.5}$$

$$e_i^- = e_j^- \tag{5.2.6}$$

Now, if e_i^- is moved to e_j^+, then the following equations can be written for the relocated network.

$$e_{ir} = e_{ir}^+ - e_{ir}^- \tag{5.2.7}$$

$$e_{jr} = e_{jr}^+ - e_{jr}^- \tag{5.2.8}$$

$$e_{ir}^- = e_{jr}^+ \tag{5.2.9}$$

Since, only e_i^+ is moved, all other node voltages remain the same and $e_{ir}^- = e_j^+$. Thus, equations 5.2.7 and 5.2.8 can be written in terms of the original network node voltages.

$$e_{ir} = e_i^+ - e_j^+ \tag{5.2.10}$$

$$e_{jr} = e_j^+ - e_j^- \tag{5.2.11}$$

Comparing equations 5.2.5 and 5.2.11, it is seen that $e_{jr} = e_j$. Also, from equation 5.2.5 and 5.2.6

$$e_j^+ = e_j + e_j^- = e_j + e_i^- \tag{5.2.12}$$

Substituting equation 5.2.12 into equation 5.2.10, e_{ir} becomes

$$e_{ir} = e_i^+ - e_j - e_i^- = (e_i^+ - e_i^-) - e_j \tag{5.2.13}$$

Finally, using equation 5.2.4 in equation 5.2.13,

$$e_{ir} = e_i - e_j$$

Thus, the ith rows of β and γ are replaced by row(i)-row(j), as a result of the relocation. The case in brackets can be proved by interchanging the roles of i and j.

As for the ideal gain of the generated network, $K_r(s)$,

$$K_r(s) = \frac{B_r'}{B_r}$$

However, B_r' and B_r are obtained from B' and B by an elementary row operation, under which the value of the determinant remains the same (ref. [32], p. 259). Therefore, the ideal gain is not altered.

5.3 Voltage Divider Method

Apart from the relocation methods, there is one other method which modifies the network, without changing the ideal gain. This method, called the voltage divider method, is generally used to stabilize an n-OA network as will be demonstrated in the applications chapter.

Theorem 5.3.1: Given an n-OA network, if the input port of any OA is modified as shown in Figure 5.3.1, then the ideal gain of the network is not affected.

Proof: The ideal gain is obtained using the ideal models of the OAs. In Figure 5.3.1, if A_i is ideal, then e_i and e_i' are both zero. If it can be shown that $\hat{e}_i$ is also zero, then the original and the modified

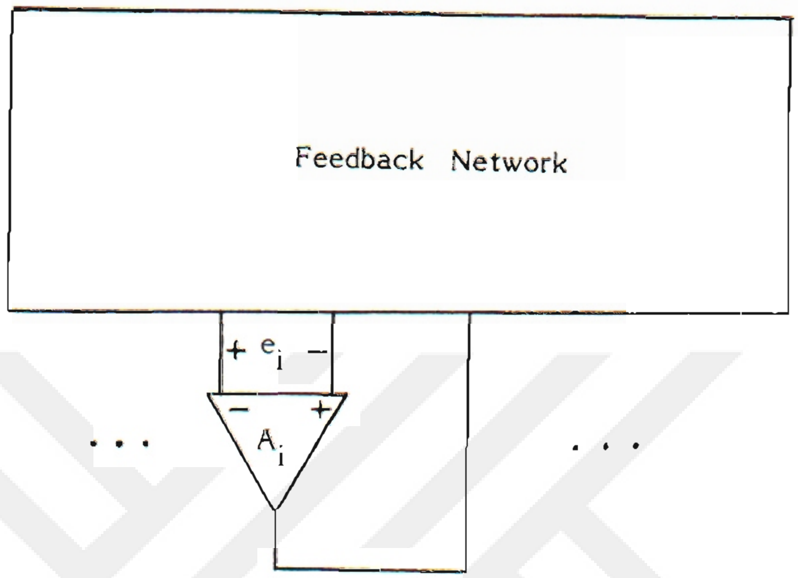

(a)

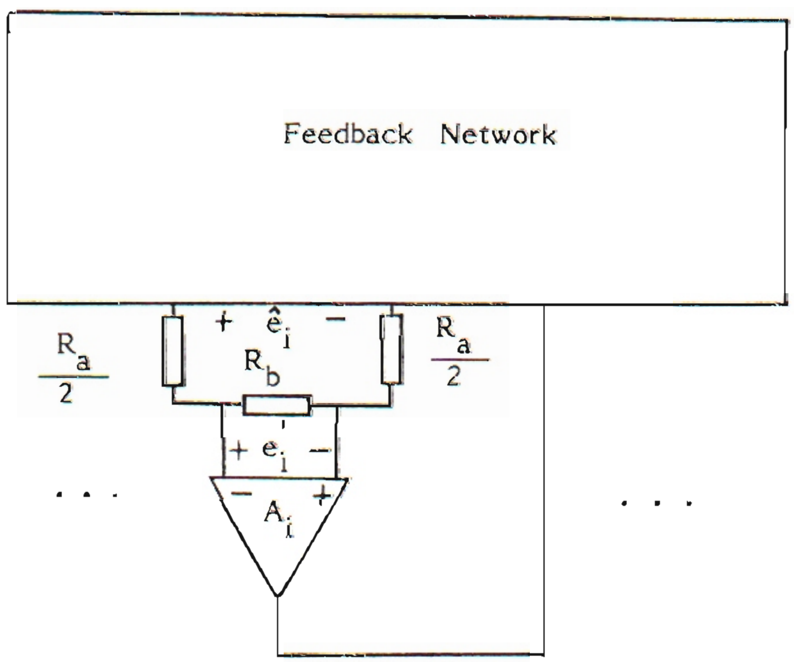

(b)

Figure 5.3.1 Voltage divider method, (a) original network, (b) modified network networks are identical in the ideal case, thus both yield the same ideal gain. In Figure 5.3.1 (b), $\hat{e}_i$ can be expressed in terms e_i',

$$\hat{e}_i = \frac{R_a + R_b}{R_b} e_i'$$

but, $e_i' = 0$ in determining the ideal gain, thus $\hat{e}_i$ is also zero. Hence, the theorem follows.

VI. NETWORKS CONTAINING n-OTAs

6.1 Introduction

The Operational Transconductance Amplifier (OTA) is another active building block which is becoming popular in network design. As the name suggests, the OTA is a voltage-controlled current-source device, whose transconductance can be adjusted externally. This feature of the OTA results in tunable active networks with fewer components. However, commercially available OTAs suffer serious limitations, such as the limited differential input voltage and the output current. Input and output buffer circuits are used to eliminate these problems.

In this chapter, first, the ideal and non-ideal characteristics of the OTA are discussed. Then, using the beta matrix approach, the general expressions for the voltage gain, input impedance, and output impedance of n-OTA networks are derived. Also, the stability and sensitivity performances of such networks are examined.

6.2 The Operational Transconductance Amplifier

The circuit symbol, along with a model for the OTA is shown in Figure 6.2.1. The terminal labelled I_{ABC} is generally not included in the circuit diagrams for simplicity. The polarity of the input voltage, u, is chosen opposite to that of the amplifier polarity to eliminate the negative signs from the system equations.

For the ideal OTA, the input impedance, r_{in}, and the output impedance, r_{out}, are infinite, and the transconductance, g_m, is independent of

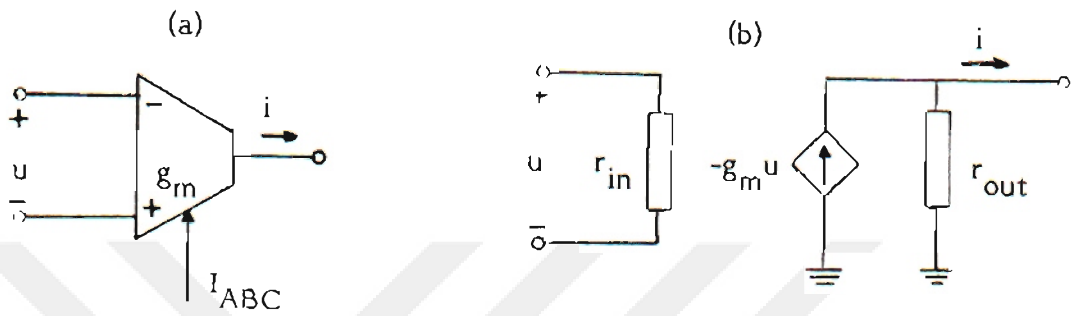

Figure 6.2.1 OTA, (a) circuit symbol, (b) model

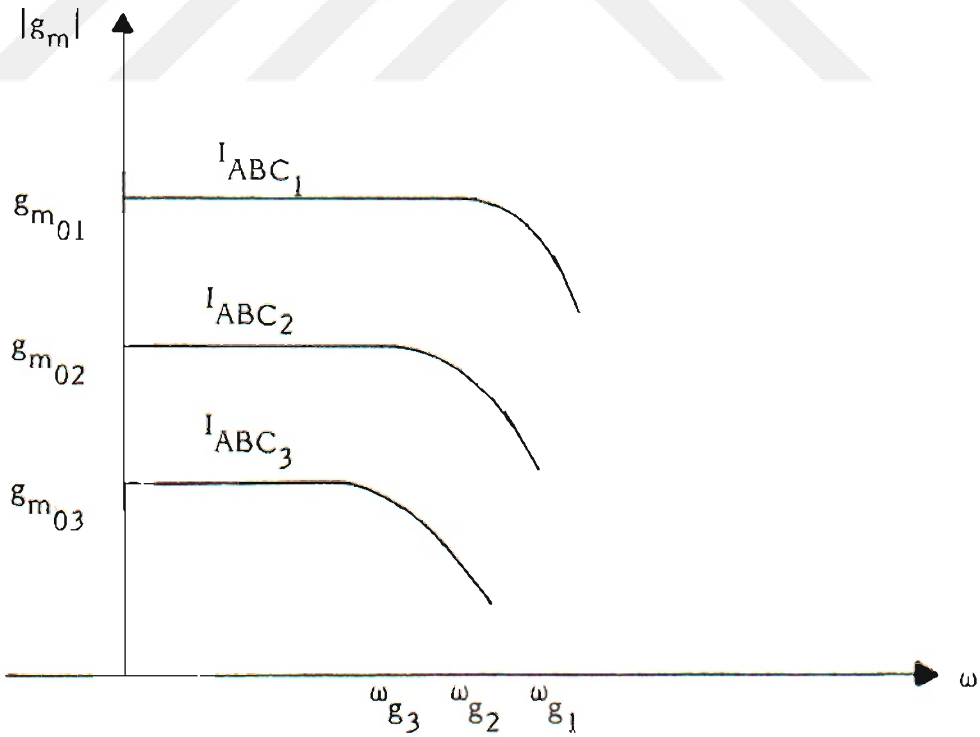

Figure 6.2.2 Transconductance magnitude vs frequency

frequency. For most applications, however, the actual behavior of these parameters are not far from ideal. The input and output impedances are very high (on the order of megaohms), and the transconductance is constant for a wide range of frequencies. The frequency response of g_m for different bias currents, I_{ABC}, is shown in Figure 6.2.2. The transconductance is controlled by varying the external bias current. g_m is directly proportional to I_{ABC} ($g_m = hI_{ABC}$), where the constant of proportionality, h, is a function for the temperature and device geometry (at room temperature h is typically between 10 - 20). The ideal value of g_m, g_{mo}, can be used for designs operating at frequencies below ω_g. However, ω_g is also a function of I_{ABC}. When g_m is varied by changing I_{ABC}, ω_g will also be varied. For this reason, it is difficult to derive a simple mathematical model for g_m. By observing the data sheets for a commonly used dual OTA chip, CA 3280, it can be seen that when g_m is varied between 30 μmhos and 30mmhos, ω_g varies between 100KHz and 10MHz respectively. As long as the operating frequency stays below the cutoff frequency, it will be assumed that g_m is independent of frequency.

6.3 Analysis of n-OTA Networks

In this section, the voltage transfer function, the input impedance and the output impedance expressions are stated in subsequent theroems. The derivation of these expressions is similar to the n-OA case and so are the proofs.

Theorem 6.3.1: Given an n-OTA network as shown in Figure 6.3.1, the transfer function is given by

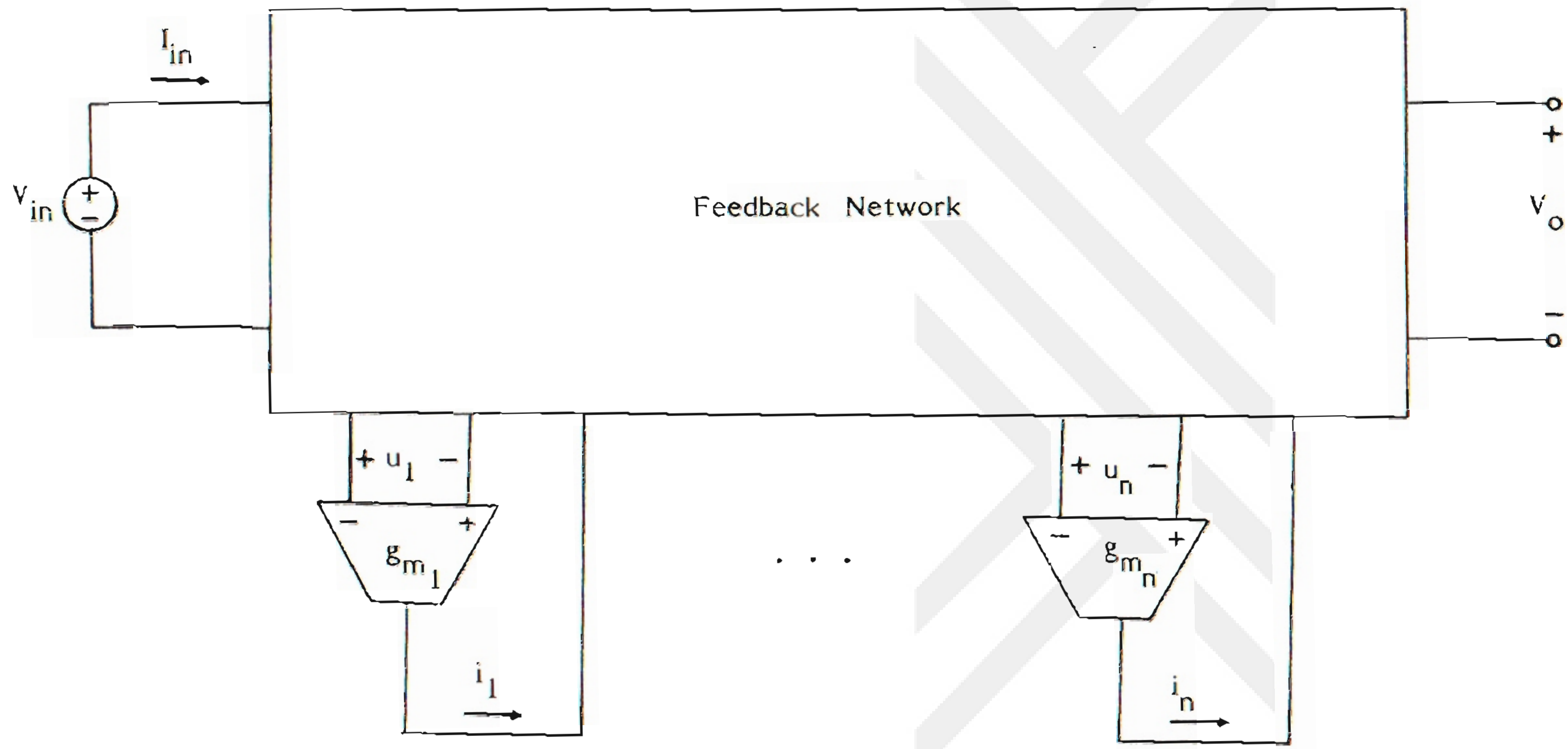

Figure 6.3.1 An n-OTA network

$$T(s) = \zeta - \alpha\,(G^{-1}+\beta)^{-1}\gamma = \frac{\det\begin{bmatrix} G^{-1}+\beta & \gamma \\ \alpha & \zeta \end{bmatrix}}{\det(G^{-1}+\beta)} \tag{6.3.1}$$

where

$$G^{-1} = \mathrm{diag}\left(\frac{1}{g_{m_1}}, \ldots, \frac{1}{g_{m_n}}\right) \tag{6.3.2}$$

$$\beta = [\beta_{ij}]_{n\times n} \quad , \quad \beta_{ij} = \left.\frac{u_i}{i_j}\right|_{\substack{i_k = V_{in} = 0 \\ k \neq j}} \tag{6.3.3}$$

$$\gamma = [\gamma_i]_{n\times 1} \quad , \quad \gamma_i = \left.\frac{u_i}{V_{in}}\right|_{i_j = 0 \quad j=1,\ldots,n} \tag{6.3.4}$$

$$\alpha = [\alpha_j]_{1\times n} \quad , \quad \alpha_j = \left.\frac{V_o}{i_j}\right|_{\substack{i_k = V_{in} = 0 \\ k \neq j}} \tag{6.3.5}$$

$$\zeta = [\zeta]_{1\times 1} \quad , \quad \zeta = \left.\frac{V_o}{V_{in}}\right|_{i_j = 0 \quad j=1,\ldots,n} \tag{6.3.6}$$

Proof: The proof is similar to the proof of Theorem 2.3.1.

Theorem 6.3.2: Given an n-OTA network as shown in Figure 6.3.1, the input impedance, $Z_{in}(s)$, is given by

$$Z_{in}(s) = \frac{1}{\zeta^{oc} - \alpha^{oc}\,(G^{-1}+\beta)^{-1}\gamma} \tag{6.3.7}$$

$$= \frac{\det(G^{-1}+\beta)}{\det\begin{bmatrix} G^{-1}+\beta & \gamma \\ \alpha^{oc} & \zeta^{oc} \end{bmatrix}} \tag{6.3.8}$$

where G^{-1}, β, and γ are as described in equations 6.3.2-6.3.4 respectively, and

$$\alpha^{oc} = [\alpha_j^{oc}]_{1xn} \quad , \quad \alpha_j^{oc} = \frac{I_{in}}{i_j}\Bigg|_{\substack{i_k = V_{in} = 0 \\ k \neq j}} \qquad (6.3.9)$$

$$\zeta^{oc} = [\zeta^{oc}]_{1x1} \quad , \quad \zeta^{oc} = \frac{I_{in}}{V_{in}}\Bigg|_{i_j = 0 \quad j=1,\ldots n} \qquad (6.3.10)$$

Proof: The proof is similar to the proof of Theorem 2.4.1.

Theorem 6.3.3: Referring to Figure 6.3.1, the output impedance, $Z_{out}(s)$, of an n-OTA network is given by

$$Z_{out}(s) = \zeta^{sc} - \alpha(G^{-1} + \beta)^{-1}\gamma^{sc} \qquad (6.3.11)$$

$$= \frac{\det \begin{bmatrix} G^{-1}+\beta & \gamma^{sc} \\ \alpha & \zeta^{sc} \end{bmatrix}}{\det (G^{-1} + \beta)} \qquad (6.3.12)$$

where G^{-1}, β, and α are given by equations 6.3.2, 6.3.3, and 6.3.5 respectively, and

$$\gamma^{sc} = [\gamma_i^{sc}]_{nx1} \quad , \quad \gamma_i^{sc} = \frac{u_i}{I_T}\Bigg|_{i_j = V_{in} = 0 \quad j=1,\ldots,n} \qquad (6.3.13)$$

$$\zeta^{sc} = [\zeta^{sc}]_{1x1} \quad , \quad \zeta^{sc} = \frac{V_T}{I_T}\Bigg|_{i_j = V_{in} = 0 \quad j=1,\ldots,n} \qquad (6.3.14)$$

Proof: The proof is similar to the proof of Theorem 2.5.1.

The ideal gain, input and output impedance expressions are obtained by replacing g_{mi}'s with g_{mio}'s.

In the next section a 3-OTA network will be analyzed to demonstrate the methods outlined in the preceeding three theorems.

6.4 Example

A 3-OTA bandpass filter is shown in Figure 6.4.1. This filter uses only two capacitors, however it should be remembered that additional circuitry is needed to supply the external bias currents for each OTA. This additional circuitry can be as simple as a resistor and as complex as a transistorized constant-current source.

The system matrices for this network can be written by observation, noting that the ith OTA output terminal is opened to make $i_i = 0$.

$$\beta = \begin{bmatrix} 0 & \frac{1}{sC_2} & 0 \\ -\frac{1}{sC_1} & 0 & -\frac{1}{sC_1} \\ \frac{1}{sC_1} & 0 & \frac{1}{sC_1} \end{bmatrix} \qquad \begin{aligned} \gamma &= [-1\ 0\ 0]^T \\ \alpha &= [\tfrac{1}{sC_1}\ \ 0\ \ \tfrac{1}{sC_1}] \\ \zeta &= [\ 0\ ] \end{aligned}$$

Thus, using equation 6.3.1, the transfer function is given by

$$T(s) = \frac{V_o}{V_{in}} = \frac{\dfrac{g_{m_1}}{C_1} s}{s^2 + \dfrac{g_{m_3}}{C_1} s + \dfrac{g_{m_1} g_{m_2}}{C_1 C_2}} \tag{6.4.1}$$

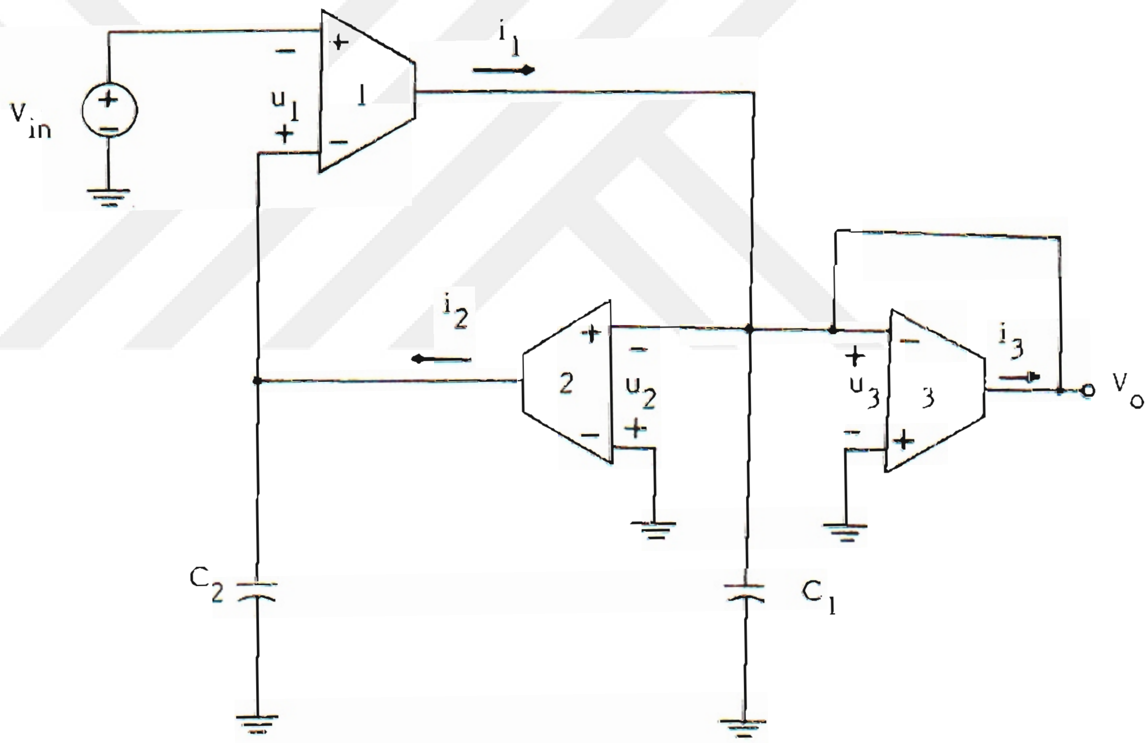

Figure 6.4.1 A 3-OTA Bandpass filter

For the input impedance,

$$\alpha^{oc} = [\ 0\ 0\ 0\ ] \quad \text{and} \quad \zeta^{oc} = [0]$$

Thus, from equation 6.3.8 the input impedance becomes

$$Z_{in}(s) = \frac{V_{in}}{I_{in}} = \infty \tag{6.4.2}$$

For the output impedance expression, the input voltage is shorted, a current source, I_T, is applied at the output, then

$$Y^{sc} = [\ 0 \ \ -\frac{1}{sC_1} \ \ \frac{1}{sC_1}\ ]^T \quad \text{and} \quad \zeta^{sc} = [\frac{1}{sC_1}]$$

Thus, from equation 6.3.12, the output impedance is given by

$$Z_{out}(s) = \frac{\frac{1}{C_1} s}{s^2 + \frac{g_{m_3}}{C_1} s + \frac{g_{m_1} g_{m_2}}{C_1 C_2}} \tag{6.4.3}$$

6.5 Stability

The transfer function expression in equation 6.3.1 is in the same form as the transfer function expression for the n-OA case, (equation 2.3.1). In equation 6.3.1 the open-loop gain matrix, A, is replaced by the transconductance matrix, G, and the entries of β and α are transresistances, and the entries of γ and ζ are voltage gains of sub-networks obtained from the passive feedback network. Hence, the stability criteria stated in Theorems 3.2.1, 3.4.1, 3.4.2, and 3.5.1, also Corollaries 3.4.1 and 3.4.2, can be adapted for the stability analysis of n-OTA networks.

The HFS test that was developed for n-OA networks, however, is not applicable to n-OTA networks for two reasons. First of all, it cannot be assumed that each OTA is identical, since the transconductance of each is used as a circuit parameter. Second the transresistance entries of the system matrices can be zero or infinity at high frequencies. Whereas the entries of the system matrices for n-OA networks are voltage gains of passive sub-networks, which approach to zero or unity at high frequencies.

6.6 Active Sensitivity

The ideal design of an n-OTA network is achieved by assuming ideal OTAs, that is the input impedance, the output impedance, and the bandwidth (BW) are assumed to be infinite. Although finite, these parameters are large enough so that the variations in the design due to them is negligible.

The input and output impedances of the OTAs are in the order of mega-ohms. Thus, if the resistors in the network are smaller than 100Kohms, then the effects of the finite input and output impedances are minimal. The BW of the OTAs varies between 100KHz and 10MHz, depending on the transconductance. In order to keep the sensitivity of the design due to the finite BW low, the design (operating) frequency must be below the BWs of the OTAs.

The transconductance at the midband frequencies, g_{mo}, is a function of temperature as well as the external bias current. The changes in g_{mo}, due to temperature and the external bias current, may effect the design parameters. The sensitivity due to these changes can be best handled by the passive sensitivity analysis (Bode sensitivities: ref. [33], pp. 113-167), treating g_m like any other passive circuit component.

VII. ACTIVE FILTER APPLICATIONS

7.1 Introduction

In this chapter two well known active filters (KHN and SB) together with other filters generated from them are examined. The stability and sensitivity methods introduced in the previous chapters are used in the analysis of these filters. Also, experimental and computer simulation data are supplied to support these calculations.

Since the evaluation of each circuit requires the repetition of similar calculations, first the step-by-step analysis method will be given. Then, the results of these calculations are summarized for each network.

7.2 Method of Analysis

In analyzing the 3-OA active filters of this chapter, the following steps are carried out:

i) <u>System Matrix:</u> The network equations are written in a matrix form as described in Chapter 2 (equation 2.3.13).

$$\begin{bmatrix} e \\ \\ V_o \end{bmatrix} = \beta' \begin{bmatrix} V \\ \\ V_{in} \end{bmatrix} \quad \text{where} \quad \beta' = \begin{bmatrix} \beta & \gamma \\ \\ \alpha & \zeta \end{bmatrix} \qquad (7.2.1)$$

In most cases the entries of β' can be written by observation using superposition of node voltages.

ii) <u>High Frequency Stability (HFS) Test:</u> When the network is designed for low frequency operation, the stability at high frequencies is governed by the OAs. If the network fails the HFS test, most probably it will remain unstable for higher operating frequency designs. Experimental data tends to support this statement.

To apply this test, first β_c is obtained from β by letting s go to infinity.

$$\beta_c = \lim_{s \to \infty} \beta \tag{7.2.2}$$

Then, the characteristic polynomial in A, $D_c(A)$, is found using equation 7.2.3.

$$D_c(A) = \det [I + \beta_c A] \tag{7.2.3}$$

It can be shown that the roots of $D_c(A)$, A_{ri}, and the eigenvalues of β_c, ρ_i', are related by

$$A_{ri} = -1/\rho_i'$$

Thus, either one can be used for the HFS Test. The network is high frequency stable if:

a) $|\underline{/A_i}| < |\underline{/A_{ri}}|$ when $|A_i| = |A_{ri}|$ (7.2.4)

or

b) $|\underline{/A_i} + \underline{/\rho_i'}| < 180°$ when $|A_i| = 1/|\rho_i'|$ (7.2.5)

Experimental data will be provided to verify the results of the HFS test.

iii) Ideal Gain and Design: The ideal gain, K, is given by

$$K = \frac{B'}{B} \tag{7.2.6}$$

where $B = \det[\beta]$ and $B' = \det[\beta']$

The ideal poles of the network are designed using the ideal gain.

iv) Poles Sensitivities: The movement of the original poles are calculated as a function of ω_o (operating frequency) and GB using equation 4.3.13. It should be remembered that this equation is derived assuming matched OAs. If otherwise, equation 4.3.10 must be used. Also, second and higher order effects of the OAs are neglected. Therefore, the sensitivity calculations (for poles and zeros) yield best results when ω_o is much lower than the GB, at least by a decade.

v) Usable Frequency Range (UFR): If the network proves to be high-frequency stable, then the next condition to examine is the movement of the design poles. In most networks, as the design frequency, ω_o, is increased, the ideal poles move towards the RHP. The circuit becomes unstable when the real part of the design poles reduces to zero.

$$\text{Re}\,[p_i] = \text{Re}\,[\Delta p_i] + \text{Re}\,[p_{io}] = 0 \tag{7.2.7}$$

or

$$\text{Re}\,[\Delta p_i] = -\,\text{Re}\,[p_{io}] \tag{7.2.8}$$

The UFR obtained is compared with the experimental data.

vi) Sensitivity of the Zeros: Since the networks analyzed in this chapter are second order BP filters, there is one ideal zero which is located at the origin. Equation 4.4.4 is used to determine the change in the ideal zero, keeping in mind that the product term in the denominator is unity when the upper limit is one. The sensitivity of the ideal zero is expressed in terms of ω_o and GB.

vii) ω_o and Q Sensitivities: The denominator of a second order BP filter determines the ω_o and Q. In addition to the design poles, parasitic poles due to the OAs are introduced into the network. If the effects of the parasitic poles are neglected, then the denominator of the network can be approximated by equation 7.2.9.

$$D(s) \cong (s-p_1)(s-p_2) = s^2 + \frac{\hat{\omega}_o}{\hat{Q}} s + \hat{\omega}_o^{\,2} \qquad (7.2.9)$$

where $p_i = p_{io} + \Delta p_i$, i=1, 2, are the actual poles, and $\hat{\omega}_o$ and $\hat{Q}$ are the actual center frequency and quality factors respectively. The variation between the ideal and actual values is caused by many factors, however only the active sensitivity, that is ω_L and GB effects, will be considered.

The results of these calculations along with the SPICE simulation results are tabulated using $\omega_L = 2\pi\,(5)$ rad/s for the OAs. $\hat{\omega}_o$ is normalized by ω_o in the tables.

viii) Comments: The filters presented will be compared in terms of their active stability and sensitivity performances.

7.3 Kerwin-Huelsman-Newcomb (KHN) Filter

The circuit diagram for the KHN filter [26] is given in Figure 2.6.1.

i) System Matrix:

$$\beta' = \begin{bmatrix} k_1 & -k_2 & k_3 & -k_4 \\ \frac{\omega_1}{s+\omega_1} & \frac{s}{s+\omega_1} & 0 & 0 \\ 0 & \frac{\omega_2}{s+\omega_2} & \frac{s}{s+\omega_2} & 0 \\ 0 & 1 & 0 & 0 \end{bmatrix} = \begin{bmatrix} \beta & \gamma \\ \alpha & \zeta \end{bmatrix} \qquad (7.3.1)$$

where

$$k_1 = \frac{G_6}{G_5 + G_6}, \quad k_2 = \frac{G_4}{G_3 + G_4}, \quad k_3 = 1 - k_1,\ k_4 = 1 - k_2,$$

$$\omega_1 = \frac{G_1}{C_1}, \quad \text{and} \quad \omega_2 = \frac{G_2}{C_2}$$

ii) HFS Test:

$$\beta = \begin{bmatrix} k_1 & -k_2 & k_3 \\ 0 & 1 & 0 \\ 0 & 0 & 1 \end{bmatrix}$$

Eigenvalues: $\rho_1' = k_1$, $\rho_2' = \rho_3' = 1$

Then, the roots of D(A) can be determined using the relation $A_{ri} = -1/\rho_i'$

$$A_{r_1} = -\frac{1}{k_1} \quad , \quad A_{r_2} = A_{r_3} = -1$$

Thus, the HFS requirements on the open-loop gains of the OAs are:

1) $|\underline{/A_i}| < 180°$ when $|A_i| = \frac{1}{k_1}$

and

2) $|\underline{/A_i}| < 180°$ when $|A_i| = 1$

These conditions are readily met by any commercially available OA.

iii) Ideal Gain and Design:

$$B' = -k_4\, \omega_1 \frac{s}{D(s)} \quad , \quad B = \frac{k_1 s^2 + k_2\omega_1 s + k_3\omega_1\omega_2}{D(s)} ,$$

$$D(s) = (s + \omega_1)(s + \omega_2)$$

Then,

$$k = -\frac{-\dfrac{k_4}{k_1}\omega_1 s}{s^2 + \dfrac{k_2}{k_1}\omega_1 s + \dfrac{k_3}{k_1}\omega_1\omega_2} = \frac{H_o \dfrac{\omega_o}{Q} s}{s^2 + \dfrac{\omega_o}{Q} s + \omega_o^2}$$

where

$$\omega_o = \sqrt{\frac{k_3}{k_1}\,\omega_1\omega_2} \quad , \quad Q = \sqrt{\frac{k_1 k_3}{k_2^2}\,\frac{\omega_2}{\omega_1}} \quad , \quad \text{and} \quad H_o = -\frac{k_4}{k_2}$$

For a design of $H_o = -99$ and $Q = 50$, pick

$$k_1 = k_3 = 0.5, \quad k_2 = 0.01, \quad k_4 = 0.99, \text{ and } \omega_1 = \omega_2 = \omega_o$$

iv) Pole Sensitivities:

$$B_{11} = \frac{s^2}{D(s)} \quad , \quad B_{22} = \frac{k_1 s(s+\omega)}{D(s)} \quad , \quad B_{33} = \frac{(k_1 s + k_2\,\omega_1)(s+\omega_2)}{D(s)}$$

$$\sum_{i=1}^{3} B_{ii} = \frac{2s^2 + 1.01\,\omega_o\,s + 0.01\,\omega_o^2}{D(s)} = C_p\,\frac{(s-s_{1p})(s-s_{2p})}{D(s)}$$

$$B = \frac{0.5\,s^2 + 0.01\,\omega_o s + 0.5\,\omega_o^2}{D(s)} = C_B\,\frac{(s-p_{10})(s-p_{20})}{D(s)}$$

Then,

$$C_p = 2 \quad , \quad s_{1p} = -0.0101\omega_o \, , \quad s_{2p} = -0.4949\,\omega_o$$

$$C_B = 0.5 \, , \; p_{10} = (-0.01 + j)\;\omega_o, \; p_{20} = p_{10}^*$$

Substituting these values into equation 4.3.13

$$\Delta p_i = \Delta p_2^* = (2.2227\ \underline{/-115.87^\circ}\,)\ [(-0.01 + j)\,\omega_o + \omega_L]\ \frac{\omega_o}{GB} \qquad (7.3.2)$$

v) Usable Frequency Range:

When $\omega_o >> \omega_L$ equation 7.3.2 can be approximated by

$$\Delta p_i \cong (2.2227 \,\underline{/\ 25.3^\circ}) \frac{\omega_o^2}{GB} \qquad (7.3.3)$$

$$Re[p_1] = -\ 0.01\ \omega_o$$

$$Re[\Delta p_1] = 2.0095\ \frac{\omega_o^2}{GB}$$

Now, using equation 7.2.8

$$\omega_{o\ max} = 0.005\ GB$$

Thus, for a GB = 1MHz, the highest design frequency before the ideal poles move into the RHP is f_o = 5KHz. The actual circuit may become unstable at a lower frequency due to the tolerances in both the active and passive components. The experimental results show that the actual UFR is approximately 10% lower than the predicted.

vi) Zero Sensitivity:

$$B'_{11} = B'_{22} = 0 \quad , \quad B'_{33} = -\ k_4\ \frac{\omega_1(s+\omega_2)}{D(s)}$$

$$\sum_{i=1}^{n} B_{ii} = -\ 0.99\omega_o\ \frac{s+\omega_o}{D(s)} = C_z\ \frac{(s-s_{1z})}{D(s)}$$

$$B' = -\ 0.99\omega_o\ \frac{s}{D(s)} = C'_B\ \frac{(s-z_{10})}{D(s)}$$

Then,

$$C_z = -0.99\ \omega_o \qquad s_{1z} = -\ \omega_o$$

$$C'_B = -0.99\ \omega_o \qquad z_{1o} = 0$$

Now, substituting these values into equation 4.4.4.

$$\Delta z_1 = -\omega_L \frac{\omega_o}{GB} \tag{7.3.4}$$

vii) <u>ω_o and Q Sensitivities:</u> The calculated and simulated values of the actual ω_o and Q are listed in Table 7.3.1.

$\frac{\omega_o}{GB}$	$\frac{\Delta p_1}{\omega_o}$	$\frac{p_1}{\omega_o}$	CALCULATED		SIMULATED	
			$\hat{\omega}_o/\omega_o$	$\hat{Q}$	$\hat{\omega}_o/\omega_o$	$\hat{Q}$
10^{-4}	2.0095×10^{-4} $-j9.4985\times10^{-5}$	-9.7990×10^{-3} $+j0.99910$	0.99995	51.021	0.99990	50.760
10^{-3}	2.0095×10^{-3} $-j9.4989\times10^{-4}$	-7.9905×10^{-3} $+j0.99905$	0.99908	62.515	0.99910	62.730
5×10^{-3}	1.0048×10^{-2} $-j4.7494\times10^{-3}$	$+4.7521\times10^{-5}$ $+j0.99525$	UNSTABLE		-	-

Table 7.3.1 KHN BP Filter with H_o=-99 and Q=50

viii) <u>Comments:</u> For a GB of 1MHz, the KHN filter center frequency can be increased up to 5KHz. The sensitivity of the center frequency is low, but as the design frequency is increased, the sensitivity of the quality factor increases.

7.4 KHN-13 Filter

In an effort to improve the performance of the KHN filter, a new network is generated (Figure 7.4.1) relocating the first and third OAs output.

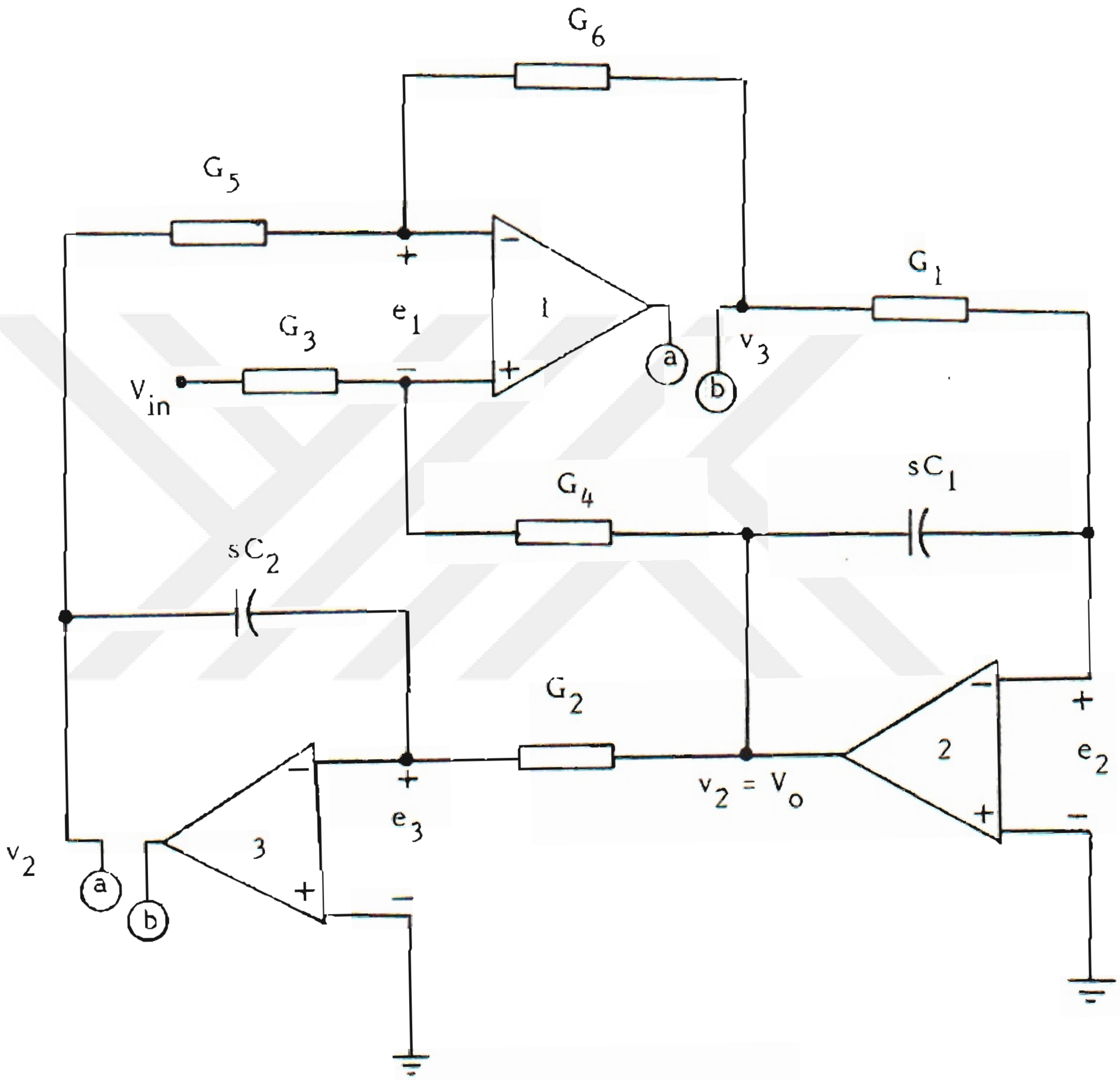

Figure 7.4.1 Output relocated KHN filter

i) System Matrix: The system matrix is obtained by interchanging the first and third columns of equation 7.3.1.

$$\beta' = \begin{bmatrix} k_3 & -k_2 & k_1 & -k_4 \\ 0 & \frac{s}{s+\omega_1} & \frac{\omega_1}{s+\omega_1} & 0 \\ \frac{s}{s+\omega_2} & \frac{\omega_2}{s+\omega_2} & 0 & 0 \\ 0 & 1 & 0 & 0 \end{bmatrix} = \begin{bmatrix} \beta & \gamma \\ \alpha & \zeta \end{bmatrix} \qquad (7.4.1)$$

ii) HFS Test:

$$\beta_c = \begin{bmatrix} k_3 & k_2 & k_1 \\ 0 & 1 & 0 \\ 1 & 0 & 0 \end{bmatrix} \qquad D(A) = -k_1(A - \frac{1}{k_1})(A+1)^2$$

Thus, the roots of D(A) are:

$$A_{r_1} = \frac{1}{k_1}, A_{r_2} = A_{r_3} = -1$$

The first root is positive, which makes the circuit unstable. The circuit was unstable when tried in the lab using a variety of OAs.

7.5 Sedra-Brown (SB) Filter

In order to make the KHN-13 filter stable, the input terminals of the third OA are reversed. The resulting network is commonly known as the SB filter [34].

i) <u>System Matrix:</u> The system matrix for the SB filter is the same as in equation 7.4.1, except the third row is negated.

ii) <u>HFS Test:</u>

$$\beta_c = \begin{bmatrix} k_3 & -k_2 & k_1 \\ 0 & 1 & 0 \\ -1 & 0 & 0 \end{bmatrix} \qquad D(A) = (A+1)[k_1 A^2 + (1-k_1)A+1]$$

Using the values selected for the KHN filter, the roots of D(A) are

$$A_{r_1} = -1, \; A_{r_2} = A^*_{r_3} = \sqrt{2} \; \underline{/110.7°}$$

Thus, the SB filter will be high-frequency stable only if

$$|\underline{/A_i}| < 110.7° \quad \text{when } |A_i| = \sqrt{2}$$

This phase of 110.7° corresponds to about 122° at the crossover frequency of an OA modelled with two poles. Not all OAs satisfy this condition, infact when this circuit was built and tested, it proved to be unstable using OAs with worse phase response (AD504's with 330pF compensation capacitors). When the same filter is tried with OAs which have a phase of 120° or less at the crossover frequency (μA741 and LM741), the network was stable.

iii) <u>Ideal Gain and Design:</u> By theorems 5.2.1 and 5.2.2 the ideal gain is the same as the KHN filter, so the same values are used for the design parameters, k_1, k_2, k_3, k_4, ω_1 and ω_2.

iv) Pole Sensitivities:

$$B_{11} = \frac{\omega_1 \omega_2}{D(s)} \;,\; B_{22} = \frac{k_1 s(s+\omega_1)}{D(s)} \;,\; B_{33} = \frac{k_3 s(s+\omega_2)}{D(s)}$$

$$\sum_{i=1}^{3} B_{ii} = \frac{s^2 + \omega_o s + \omega_o^2}{D(s)} = C_p \frac{(s-s_{1p})(s-s_{2p})}{D(s)}$$

$$B = \frac{0.5s^2 + 0.01\,\omega_o s + 0.5\omega_o^2}{D(s)} = C_B \frac{(s-p_{10})(s-p_{20})}{D(s)}$$

$$C_p = 1 \;,\; s_{1p} = (-0.5 + j\,0.8666)\,\omega_o \;,\; s_{2p} = s_{1p}^*$$

$$C_B = 0.5 \;,\; p_{10} = (-0.01 + j)\,\omega_o, \;\; p_{20} = p_{10}^*$$

Now, using equation 4.3.13

$$\Delta p_1 = (0.9801 \;\underline{/ -179.42^\circ}\,)\,[\,(-0.01 + j)\omega_o + \omega_L]\,\frac{\omega_o}{GB} \tag{7.5.1}$$

v) Usable Frequency Range: When $\omega_o >> \omega_L$, equation 7.5.1 can be approximated as

$$\Delta p_1 \simeq (0.9801 \;\underline{/-88.85^\circ}\,)\,\frac{\omega_o^2}{GB}$$

$$Re[p_1] = -\,0.01\,\omega_o \tag{7.5.2}$$

$$Re[\Delta p_1] = 0.01967\,\frac{\omega_o^2}{GB}$$

Thus, by equation 7.2.8, the UFR is given by

$$\omega_{o_{max}} = 0.5084\ GB$$

Experimental results showed that the network was stable up to $\omega_o = 2\pi\,(24000)$ rad/s using OAs with GBs of 900KHz. There is a considerable difference in the experimental and theoretical UFRs, since UFR calculation considers the movement of the ideal poles only. However, because the OAs used barely meet the HFS condition, as ω_o is increased the parasitic poles move into the unstable half of the complex plane, before the ideal poles. Therefore, in designing active networks, as a rule of thumb, a phase margin of 45° should be allowed in satisfying the HFS criterion.

vi) Zero Sensitivity:

$$B'_{11} = B'_{22} = B'_{33} = 0$$

Thus, $\Delta z_1 = 0$, i.e. the ideal zero is not affected by the OAs.

vii) ω_o and Q Sensitivities: The calculated and simulated values of the actual ω_o and Q are listed in Table 7.3.2.

$\frac{\omega_o}{GB}$	$\frac{\Delta p_1}{\omega_o}$	$\frac{p_1}{\omega_o}$	CALCULATED		SIMULATED	
			$\hat{\omega}_o/\omega_o$	$\hat{Q}$	$\hat{\omega}_o/\omega_o$	$\hat{Q}$
10^{-4}	1.9671×10^{-6} $-j9.7990\times10^{-5}$	-9.9980×10^{-3} $+j9.9990\times10^{-1}$	0.9995	50.0049	0.99995	50.25
10^{-3}	1.9671×10^{-5} $-j9.7990\times10^{-4}$	-9.9803×10^{-3} $+j9.9902\times10^{-1}$	0.99907	50.0495	0.9989	50.20
10^{-2}	1.9671×10^{-4} $-j9.7990\times10^{-3}$	-9.8033×10^{-3} $+j9.9020\times10^{-1}$	0.99025	50.5035	0.9905	51.86
10^{-1}	1.9671×10^{-3} $-j9.7990\times10^{-2}$	-8.0329×10^{-3} $+j9.0201\times10^{-1}$	0.90205	56.1444	0.92180	413.36

Table 7.3.2 SB BP Filter with $H_o = -99$ and $Q = 50$

This large difference between the calculated and simulated values when $\omega_o = 0.1$ GB, also suggests that the parasitic poles begin showing their effects on the frequency response. As a matter of fact the network became unstable at this frequency when tested in the lab.

viii) Comments: ω_o and Q sensitivities, as well as the UFR shows remarkable improvements over the KHN filter. However, this filter is stable only for those OAs satisfying the HFS criterion.

In order to relax the HFS condition of the SB filter, the voltage divider technique of Chapter 5 will be used in the next section.

7.6 Modified SB (M-SB) Filter

In the SB filter, the third OA has no direct feedback path from its output to its input. That is, the third OA acts like an open-loop amplifier causing the poor HFS condition. To improve the HFS, the voltage-divider technique of Chapter 5 is used. The resulting network is called the Modified-SB (M-SB) filter. The modified portion of the network is shown in Figure 7.6.1.

i) System Matrix:

$$\beta' = \begin{bmatrix} k_3 & -k_2 & k_1 & -k_4 \\ 0 & \frac{s}{s+\omega_1} & \frac{\omega_1}{s+\omega_1} & 0 \\ -k\frac{s}{s+\omega_3} & -k\frac{\omega_2}{s+\omega_3} & 0 & 0 \\ 0 & 1 & 0 & 0 \end{bmatrix} = \begin{bmatrix} \beta & \gamma \\ \alpha & \zeta \end{bmatrix}$$

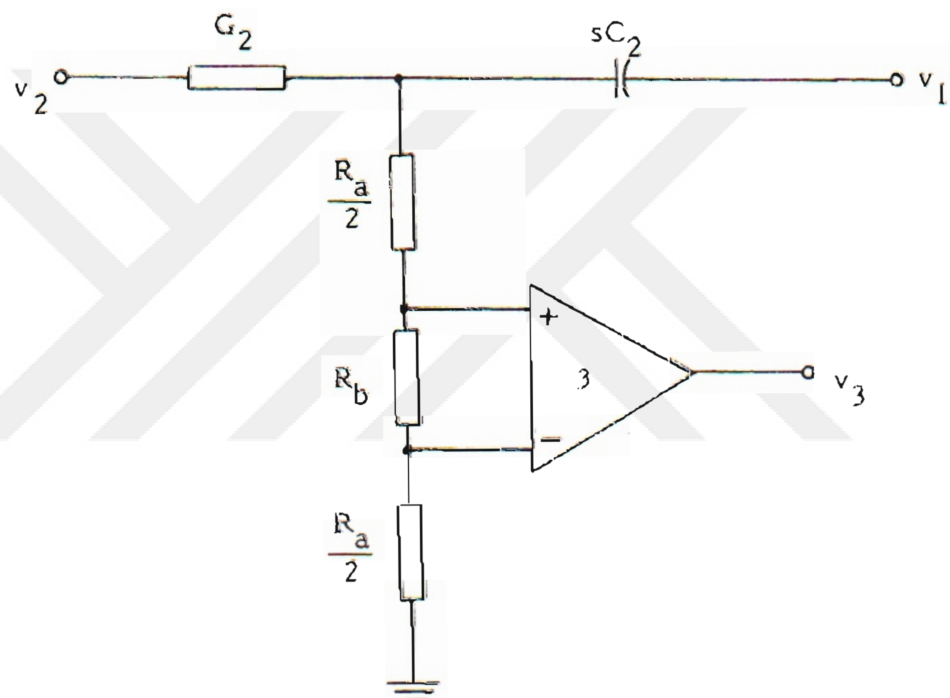

Figure 7.6.1 Modified portion of the M-SB filter

where

$$\omega_3 = \omega_2 + \Delta\omega_2 \quad , \Delta\omega_2 = \frac{G}{C_2}, \quad G = \frac{1}{R_a + R_b} \quad , \quad k = \frac{R_b}{R_a + R_b}$$

ii) <u>HFS Test:</u>

$$\beta_c = \begin{bmatrix} k_3 & -k_2 & k_1 \\ 0 & 1 & 0 \\ -k & 0 & 0 \end{bmatrix} \qquad D(A) = (A+1)[kk_1 A^2 + (1-k_1)A + 1]$$

If $k_1 = \frac{1}{2}$ and $k = \frac{1}{2}$, then the roots of D(A) are:

$$A_{r_1} = -1 \qquad A_{r_2} = 2\ \underline{/120°} \quad \text{and} \quad A_{r_3} = 2\ \underline{/-120°}$$

Thus, compared to the SB filter, M-SB filter has an improved HFS criterion:

$$|\,\underline{/A_i}\,| < 120° \qquad \text{when } |A_i| = 2$$

This phase of 120° corresponds to 134° at the crossover frequency. Most OAs satisfy this condition. However, when the circuit was tried using k= 1/2 and AD504 with 330pF compensation capacitors the circuit was still unstable. This unstability is due to the fact that these OAs have a measured phase of 150° or more at the crossover frequency. The network can still be made stable by reducing k. If k is made 1/8, then the three roots of D(A) are real and negative, in which case the HFS is independent of the OAs used. When the M-SB filter was tested with 1:8 voltage divider, the network was stable, but the UFR and active sensitivities became worse.

It seems that HFS, UFR, and sensitivities are indirectly proportional to each other, that is the designer has to sacrifice one to improve the other.

iii) Ideal Gain and Design: By theorem 5.3.1, the ideal gain is not affected by the modification. The design is realized using $k = \frac{1}{2}$, $\Delta\omega_2 = \omega_o/20$, and the same values for the rest of the parameters. Eventhough the magnitude of $\Delta\omega_2$ does not change the HFS criterion and it has little effect on the sensitivities, it does affect the UFR. As $\Delta\omega_2$ is made smaller, the UFR increases.

iv) Pole Sensitivities:

$$B_{11} = \frac{k\omega_1\omega_2}{D(s)}, \quad B_{22} = \frac{kk_1 s(s+\omega_1)}{D(s)}, \quad B_{33} = \frac{k_3 s(s+\omega_3)}{D(s)}, \quad D(s) = (s+\omega_1)(s+\omega_3)$$

$$\sum_{i=1}^{3} B_{ii} = \frac{0.75s^2 + 0.775\omega_o s + 0.5\omega_o^2}{D(s)} = C_p \frac{(s-s_{1p})(s-s_{2p})}{D(s)}$$

$$B = 0.5 \frac{0.5s^2 + 0.01\omega_o s + 0.5\omega_o^2}{D(s)} = C_B \frac{(s-p_{10})(s-p_{20})}{D(s)}$$

$C_p = 0.75$, $s_{1p} = (-0.5167 + j0.6322)\,\omega_o$, $s_{2p} = s_{1p}^*$

$C_B = 0.25$, $p_{10} = (-0.01 + j)\omega_o$, $p_{20} = p_{10}^*$

Substituting these values in equation 4.3.13

$$\Delta p_1 = (1.6051 \underline{/-161.27^\circ})\ [(-0.01 + j)\omega_o + \omega_L]\ \frac{\omega_o}{GB} \qquad (7.6.1)$$

v) Usable Frequency Range: Making the same approximation as before equation 7.6.1 becomes

$$\Delta p_1 \simeq (1.6051 \underline{/-70.7^\circ})\ \frac{\omega_o^2}{GB} \qquad (7.6.2)$$

Then, the UFR is:

$$\omega_{omax} = 0.0188\ GB \qquad (7.6.3)$$

Using OAs with GBs of around 900KHz, the UFR, according to equation 7.6.3, is around 16.9KHz. The experimental results yield a UFR of 11.3KHz. This difference may have been caused by the mismatching of the OAs; since the calculations above assume matched OAs.

vi) Zero Sensitivity:

$$B'_{11} = B'_{22} = B'_{33} = 0$$

Thus, $\Delta z_1 = 0$, implying that the ideal zero stays at the origin.

vii) ω_o and Q Sensitivities: The calculated and simulated values of the actual ω_o and Q are listed in Table 7.3.3.

$\frac{\omega_o}{GB}$	$\frac{\Delta p_1}{\omega_o}$	$\frac{p_1}{\omega_o}$	CALCULATED		SIMULATED	
			$\hat{\omega}_o/\omega_o$	$\hat{Q}$	$\hat{\omega}_o/\omega_o$	$\hat{Q}$
10^{-4}	5.31×10^{-5} $-j1.51\times10^{-4}$	-9.95×10^{-3} $+j9.998\times10^{-1}$	0.99990	50.26	0.9999	50.00
10^{-3}	5.31×10^{-4} $-j1.51\times10^{-3}$	-9.47×10^{-3} $+j9.92\times10^{-1}$	0.99853	52.72	0.9925	53.11
10^{-2}	5.31×10^{-3} $-j1.51\times10^{-2}$	-4.69×10^{-3} $+j9.85\times10^{-1}$	0.98486	104.88	0.9853	107.10

Table 7.3.3 M-SB Filter with $H_o = -99$ and $Q = 50$

viii) Comments: Eventhough the sensitivity performance of the filter is degraded with the voltage divider modification, the HFS criterion is relaxed, i.e. the phase requirement of the open-loop gain of the OAs used in the circuit can be satisfied by more OAs.

The value of k is 1 for the SB filter and $\frac{1}{2}$ for the M-SB filter; k=1 creates HFS problems (at high frequencies) and k < 1 causes a drop in the sensitivites (at the design frequency, ω_o). If a frequency varying voltage divider can be used such that around the design frequency k=1 and at high frequencies $k=\frac{1}{2}$ or less, then the sensitivity performance can be improved and the HFS criterion can be kept the same. In the next section such a voltage divider will be employed.

7.7 Compensated - SB (CSB) Filter

The compensated voltage divider replacing the resistive voltage divider of the M-SB filter is shown in Figure 7.7.1. For this network:

$$e_3 = -k\frac{s+\omega_b}{s+k\omega_b}v, \quad \text{where} \quad k = \frac{R_b}{R_a+R_b} \quad \text{and} \quad \omega_b = \frac{1}{R_bC_b} \qquad (7.7.1)$$

As can be seen from equation 7.7.1, at high frequencies $e_3 = -kv$ and at frequencies much less than $k\omega_b$, $e_3 = -v$.

i) System Matrix:

$$B' = \begin{bmatrix} k_3 & -k_2 & k_1 & k_4 \\ 0 & \frac{s}{s+\omega_1} & \frac{\omega_1}{s+\omega_1} & 0 \\ \frac{-ks(s+\omega_b)}{D_1} & \frac{-k\omega_2(s+\omega_b)}{D_1} & 0 & 0 \\ 0 & 1 & 0 & 0 \end{bmatrix}$$

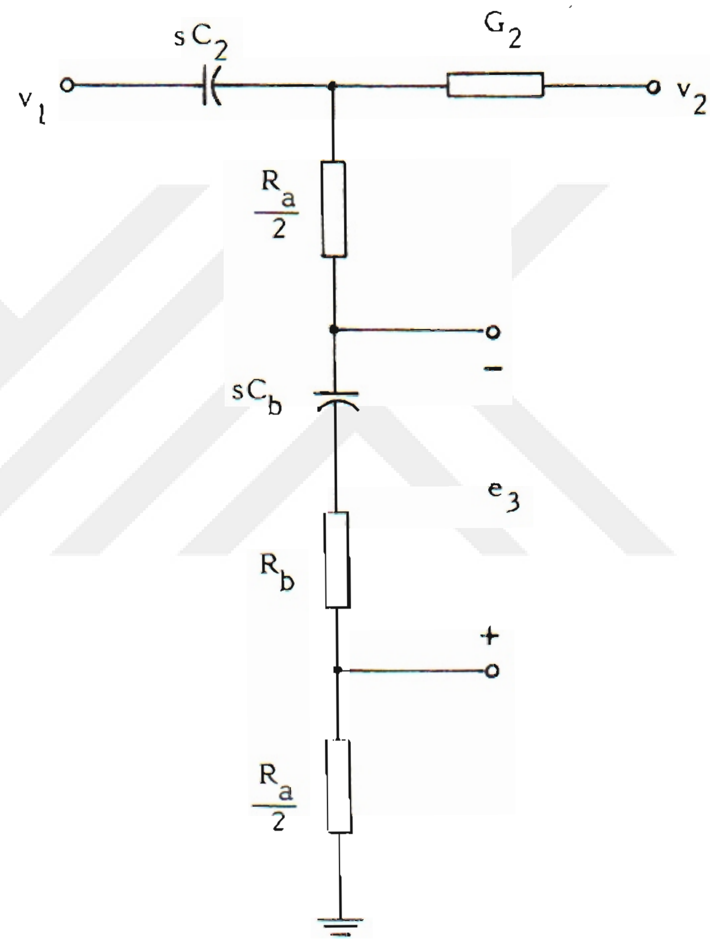

Figure 7.7.1 Compensated voltage divider

where $D_1 = s^2 + (\omega_3 + k\,\omega_b)\,s + k\,\omega_b\,\omega_2$

ii) HFS Test: The results of this test are not affected by the compensation. When this network was tested in the lab using OAs with a phase of 130° or less, it was stable and the UFR was increased.

iii) Ideal Gain and Design:

$$B' = \frac{-k\,k_4\omega_1 s(s+\omega_b)}{D(s)}$$

$$B = k\,\frac{[k_1 s^2 + k_2\omega_1 s + k_3\omega_1\omega_2]\,(s+\omega_b)}{D(s)}$$

where

$$D(s) = D_1(s+\omega_1)$$

Then, the ideal gain is:

$$k = \frac{B'}{B} = \frac{-\dfrac{k_4}{k_1}\,\omega_1 s}{s^2 + \dfrac{k_2}{k_1}\omega_1 s + \dfrac{k_3}{k_1}\,\omega_1\omega_2}$$

Thus, the ideal gain remains the same for all the four networks examined: KHN, SB, M-SB, and C-SB.

The only new variable in the design is ω_b. To eliminate the effects of the voltage divider on ω_o and Q, pick $k\,\omega_b >> \omega_o$. For the following calculations, $k\,\omega_b = 10\,\omega_o$. The values for the rest of the parameters are kept the same.

iv) Pole Sensitivities:

$$B_{11} = \frac{k\,\omega_1\,\omega_2(s+\omega_b)}{D(s)}\ , \quad B_{22} = \frac{kk_1 s(s+\omega_b)(s+\omega_1)}{D(s)}\ , \quad B_{33} = \frac{k_3 s\, D_1}{D(s)}$$

$$\sum_{i=1}^{3} B_{ii} = \frac{0.75s^3+10.775\,\omega_o s^2 + 10.5\omega_o^2 s + 10\omega_o^3}{D(s)} = C_p\,\frac{(s-s_{1p})(s-s_{2p})(s-s_{3p})}{d(s)}$$

$$B = 0.5\,\frac{(0.5s^2+0.01\,\omega_o s+0.5\omega_o^2)(s+20\omega_o)}{D(s)} = C_B\,\frac{(s-p_{10})(s-p_{20})(s-p_{30})}{D(s)}$$

$C_p = 0.75$, $s_{1p} = (-0.4854 + j0.8716)\,\omega_o$, $s_{2p} = s_{1p}^*$, $s_{3p} = -13.4\,\omega_o$

$C_B = 0.25$, $p_{10} = (-0.01 + j)\,\omega_o$, $p_{20} = p_{10}^*$, $p_{30} = -20\omega_o$

Now, using these values in equation 4.3.13

$$\Delta p_1 = (0.9569\ \underline{/-177.73°}\ )\ [(-0.01 + j)\,\omega_o + \omega_L]\ \frac{\omega_o}{GB} \qquad (7.7.2)$$

v) Usable Frequency Range: When $\omega_o >> \omega_L$, equation 7.7.2 can be approximated by

$$\Delta p_1 \simeq (0.9569)\underline{/-87.16°}\ \ \frac{\omega_o^2}{GB} \qquad (7.7.3)$$

Then, the UFR is given by

$$\omega_{omax} = 0.21GB \qquad (7.7.4)$$

In the lab when OAs with GBs around 900KHz were used, the C-SB filter was stable up to $\omega_o = 2\pi\,(50KHz)$ which is about 0.056 GB. The difference between the predicted and experimental UFRs may be due to the parasitic poles. The HFS phase requirement is met by a margin of 15° with the OAs used, and apparently, to minimize the effects of the parasitic poles, this margin needs to be increased.

vi) Zero Sensitivity:

$$B'_{11} = B'_{22} = B'_{33} = 0$$

thus, $\Delta z_1 = 0$

vii) ω_o and Q Sensitivities: The calculated and simulated values of the actual ω_o and Q are listed in Table 7.3.4.

$\frac{\omega_o}{GB}$	$\frac{\Delta p_1}{\omega_o}$	$\frac{p_1}{\omega_o}$	CALCULATED		SIMULATED	
			$\hat{\omega}_o/\omega_o$	$\hat{Q}$	$\hat{\omega}_o/\omega_o$	$\hat{Q}$
10^{-4}	4.74×10^{-6} $-j9.56\times10^{-5}$	-9.995×10^{-3} $+j9.999\times10^{-1}$	0.99995	50.02	0.9999	50.25
10^{-3}	4.74×10^{-5} $-j9.56\times10^{-4}$	-9.953×10^{-3} $+j9.990\times10^{-1}$	0.99909	50.19	0.9991	50.46
10^{-2}	4.74×10^{-4} $-j9.56\times10^{-3}$	-9.526×10^{-3} $+j9.904\times10^{-1}$	0.99049	51.99	0.9907	53.26
5×10^{-2}	2.37×10^{-3} $-j4.78\times10^{-2}$	-7.63×10^{-3} $+j9.52\times10^{-1}$	0.95224	62.40	0.9582	93.94

Table 7.3.4 C-SB BP Filter with H_o=-99 and Q=50

viii) Comments: When the C-SB filter is compared to the SB filter, the ω_o and Q sensitivities are slightly higher. However, because of the improved HFS condition, the actual UFR is doubled, eventhough the predicted

UFR is lower in the C-SB network.

7.8 Mikhael-Bhattacharyya (MB) Filter

The second filter which will be examined is a popular 3-OA biquad, commonly known as the MB Filter (Figure 7.8.1) [18].

i) System Matrix:

$$\beta' = \begin{bmatrix} h_1 & h_2 & (h_3 - k_1) & 0 \\ (h_1 - k_2) & h_2 & h_3 & -k_3 \\ h_1 & (h_2 - \frac{s}{s+\omega_2}) & h_3 & 0 \\ 0 & 0 & 1 & 0 \end{bmatrix} = \begin{bmatrix} \beta & \gamma \\ \alpha & \zeta \end{bmatrix}$$

where

$$h_1 = \frac{\omega_1'}{s+\omega_1}, \quad h_2 = \frac{\omega_1''}{s+\omega_1}, \quad h_3 = \frac{s}{s+\omega_1}, \quad k_1 = \frac{G_7}{G_2+G_7}, \quad k_2 = \frac{G_9}{G_3+G_4+G_9},$$

$$k_3 = \frac{G_3}{G_3+G_4+G_9}, \quad \omega_1 = \omega_1' + \omega_1'', \quad \omega_1' = \frac{G_8}{C_1}, \quad \omega_1'' = \frac{G_{10}}{C_1}, \text{ and } \omega_2 = \frac{G_6}{C_2}$$

ii) HFS Test:

$$\beta_c = \begin{bmatrix} 0 & 0 & (1-k_1) \\ -k_2 & 0 & 1 \\ 0 & -1 & 1 \end{bmatrix} \quad D(A) = k_2(1-k_1)A^3 + A^2 + A + 1$$

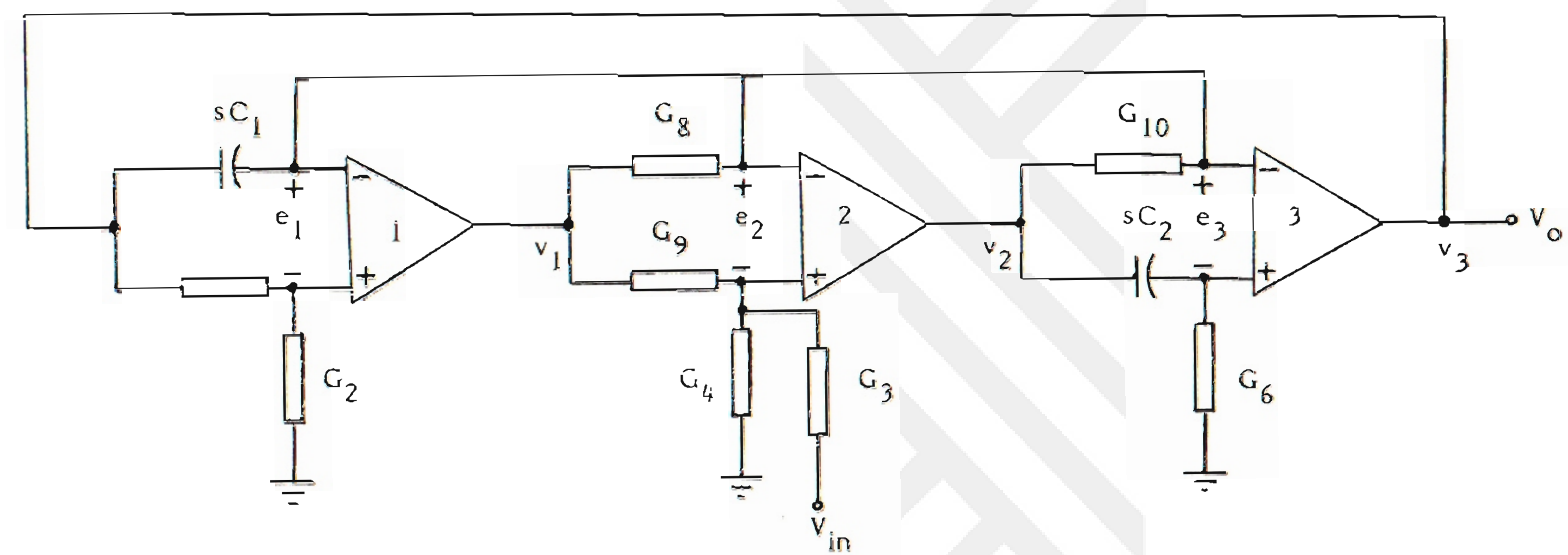

Figure 7.8.1 MB Bandpass filter

As $k_2(1-k_1)$ is varied between 0 and 1, the complex roots of D(A) varies between $\underline{1/\pm120°}$ and $\underline{1/\pm90°}$, while the real root varies between $-\infty$ and -1. So, the HFS condition at best (when $k_2(1-k_1)= 0$) requires OAs with a phase less than 120° at the crossover frequency. The MB filter was tried using $k_1=0.5$, $k_2=0.8761$ and OAs with a phase of 120° each and was found to be unstable. The roots of D(A) at these values of k_1 and k_2 are

$$A_{r_1} = -1.729 \quad A_{r_2} = 1.15\underline{/104°} \text{ and } A_{r_3} = 1.15\underline{/-104°}$$

Thus, the HFS suggests that, the OAs used must possess the following condition:

$$|\underline{/A_i}| < 104° \text{ when } |A_i| = 1.15$$

Assuming that this condition is satisfied, the analysis is continued.

iii) <u>Ideal Gain and Design:</u>

$$B' = \frac{k_3\omega_1' s}{D(s)}$$

$$B = \frac{k_2(1-k_1)s^2+k_1(1-k_2)\omega_1' s+k_1k_2\omega_1''\omega_2}{D(s)}$$

where $D(s) = (s+\omega_1)(s+\omega_2)$

Then,

$$K = \frac{B'}{B} = \frac{H_o\frac{\omega_o}{Q}s}{s^2+\frac{\omega_o}{Q}s+\omega_o^2}$$

where

$$\omega_o = \sqrt{\frac{k_1}{1-k_1}\,\omega_1''\,\omega_2} \quad , \quad Q = \frac{k_2}{1-k_2}\sqrt{\frac{1-k_1}{k_1}\,\frac{\omega_1''\,\omega_2}{\omega_1'^2}}\,, \text{ and } H_o = \frac{k_3}{k_1(1-k_2)}$$

For a design of $H_o = 1$ and $Q = 50$, pick $\omega_1'' = \omega_2 = \omega_o$, $k_1 = 0.5$, and $\omega_1' = \omega_o / \sqrt{50}$; then $k_2 = 0.8761$ and $k_3 = 0.06195$

iv) Pole Sensitivities:

$$B_{11} = \frac{s^2}{D(s)} \quad , \quad B_{22} = \frac{k_1\omega_1'(s+\omega_2)}{D(s)} \quad , \quad B_{33} = \frac{k_2\omega_1''(s+\omega_2)}{D(s)}$$

$$\sum_{i=1}^{n} B_{ii} = \frac{s^2+0.9468\omega_o s + 0.9468\omega_o^2}{D(s)} = C_p\,\frac{(s-s_{1p})(s-s_{2p})}{D(s)}$$

$$B = 0.43805\,\frac{s^2+0.02\omega_o s+\omega_o^2}{D(s)} = C_B\,\frac{(s-p_{10})(s-p_{20})}{D(s)}$$

where

$$C_p = 1 \,,\ s_{1p} = (-0.4734 + j\,0.8501)\omega_o \,,\ s_{2p} = s_{1p}^*$$

$$C_B = 0.43805 \quad , \quad p_{10} = (-0.01 + j)\,\omega_o,\ p_{20} = p_{10}^*$$

Using equation 4.3.13 with the values above,

$$\Delta p_1 = (1.0603 \,\underline{/-176.14^\circ}\,)\,[(-0.01 + j)\,\omega_o + \omega_L]\,\frac{\omega_o}{GB} \qquad (7.8.1)$$

v) Usable Frequency Range: When $\omega_o >> \omega_L$, equation 7.8.1 is approximated by equation 7.8.2:

$$\Delta p_1 = (1.0603\,\underline{/-85.57^\circ})\,\frac{\omega_o^2}{GB} \qquad (7.8.2)$$

Thus, the UFR is

$$\omega_{omax} = 0.122 \text{ GB} \tag{7.8.3}$$

vi) Zero Sensitivity:

$$B'_{11} = k_3 \frac{s^2 + \omega'_1 s + \omega''_1 \omega_2}{D(s)} \quad , \quad B'_{22} = B'_{33} = 0$$

$$\sum_{i=1}^{3} B'_{ii} = k_3 \frac{s^2 + 0.1414s - \omega_o^2}{D(s)} = C_z \frac{(s-s_{1z})(s-s_{2z})}{D(s)}$$

$$B' = 0.1414\, k_3 \omega_o \frac{s}{D(s)} = C'_B \frac{s-z_{10}}{D(s)}$$

$$C_z = k_3, \quad s_{1z} = 0.9318\omega_o \, , \, s_{2z} = -1.0732\omega_o$$

$$C'_B = 0.1414 k_3 \omega_o \quad , \, z_{10} = 0$$

Now, using these values in equation 4.4.4

$$\Delta z_1 = 0.1414\, \omega_L \frac{\omega_o}{GB}$$

Thus, the ideal zero move towards the RHP as the center frequency is increased.

vii) ω_o and Q Sensitivities: The calculated and simulated values of the actual ω_o and Q are listed in Table 7.3.5.

$\frac{\omega_o}{GB}$	$\frac{\Delta p_1}{\omega_o}$	$\frac{p_1}{\omega_o}$	CALCULATED $\hat{\omega}_o/\omega_o$	CALCULATED $\hat{Q}$	SIMULATED $\hat{\omega}_o/\omega_o$	SIMULATED $\hat{Q}$
10^{-4}	8.19×10^{-6} $-j1.06\times10^{-4}$	-9.99×10^{-3} $+j9.999\times10^{-1}$	0.99994	50.04	0.9999	50.00
10^{-3}	8.19×10^{-5} $-j1.06\times10^{-3}$	-9.92×10^{-3} $+j9.989\times10^{-1}$	0.99899	50.36	0.9990	50.20
10^{-2}	8.19×10^{-4} $-j1.06\times10^{-2}$	-9.18×10^{-3} $+j9.894\times10^{-1}$	0.98947	53.88	0.9896	54.37
10^{-1}	8.19×10^{-3} $-j1.06\times10^{-1}$	-1.81×10^{-3} $+j8.943\times10^{-1}$	0.89429	247.02	0.9066	106.66

Table 7.3.5 MB BP Filter with $H_o = 1$ and $Q = 50$

viii) Comments: The stringent HFS criterion can only be satisfied by a limited number of OAs, making this filter unattractive, inspite of the low ω_o and Q sensitivities.

7.9 Output Relocated MB (OR-MB) Filter

When the first and second OA outputs are interchanged and the input terminals of the second OA are reversed, a new filter, OR-MB, is generated (Figure 7.9.1).

i) System Matrix:

$$\beta' = \begin{bmatrix} h_2 & h_1 & (h_3-k_1) & 0 \\ -h_2 & (k_2-h_1) & -h_3 & -k_3 \\ (h_2-\frac{s}{s+\omega_2}) & h_1 & h_3 & 0 \\ 0 & 0 & 1 & 0 \end{bmatrix} = \begin{bmatrix} \beta & \gamma \\ \alpha & \zeta \end{bmatrix}$$

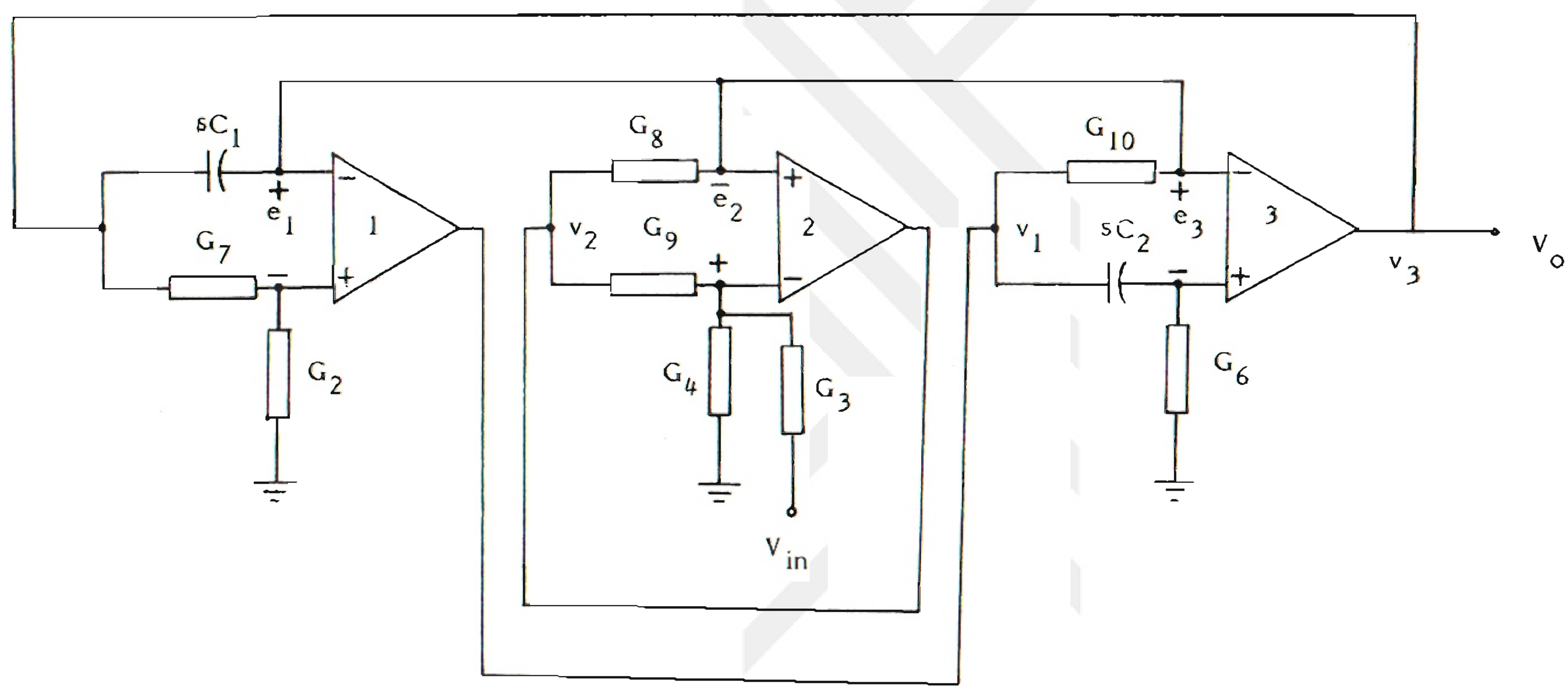

Figure 7.9.1 OR-MB Bandpass filter

ii) HFS Test:

$$\beta_c = \begin{bmatrix} 0 & 0 & (1-k_1) \\ 0 & k_2 & -1 \\ -1 & 0 & 1 \end{bmatrix} \quad D(A) = (1-k_1)k_2A^3+(1+k_2-k_1)A^2+(1+k_2)A+1$$

using the previously selected values (k_1=0.5 and k_2=0.8761), the roots of D(A) are

$$A_{r_1} = -1.1414 \quad A_{r_2} = \sqrt{2}\ \underline{/135°} \quad A_{r_3} = \sqrt{2}\ \underline{/-135°}$$

Then, the HFS criterion is:

$$|\underline{/A_i}| < 135° \qquad \text{when} \quad |A_i| = \sqrt{2}$$

The phase at the crossover frequency needs to be less than about 142°. This condition is easier to satisfy.

iii) Ideal Gain and Design: By theorems 5.2.1 and 5.2.2 the ideal gain remains the same as the original network. The same design values picked for the MB filter will be used.

iv) Pole Sensitivites:

$$B_{11} = \frac{k_2 s(s+\omega_2)}{D(s)}, \quad B_{22} = \frac{(1-k_1)s^2-k_1\omega_1' s + k_1\omega_1''\omega_2}{D(s)}, \quad B_{33} = \frac{k_2\omega_1''(s+\omega_2)}{D(s)}$$

$$\sum_{i=1}^{3} B_{ii} = 1.3761\,\frac{s^2+1.2219\omega_o s+\omega_o^2}{D(s)} = C_p\,\frac{(s-s_{1p})(s-s_{2p})}{D(s)}$$

$$B = 0.43805\,\frac{s^2+\ 0.02\omega_o s + \omega_o^2}{D(s)} = C_B\,\frac{(s-p_{10})(s-p_{20})}{D(s)}$$

where

$$C_p = 1.3761 \ , \ s_{1p} = (-0.6110 + j\,0.7917)\,\omega_o \ , \ s_{2p} = s_{1p}^*$$

$$C_B = 0.43805 \ , \ p_{10} = (-0.01 + j)\,\omega_o \ , \ p_{20} = p_{10}^*$$

Thus,

$$\Delta p_1 = (1.8881 \ \underline{/-179.43^\circ}\ )\,[\,(-0.01 + j)\omega_o + \omega_L\,]\,\frac{\omega_o}{GB} \qquad (7.9.1)$$

v) Usable Frequency Range: When $\omega_o >> \omega_L$, equation 7.9.1 can be approximated as

$$\Delta p_1 \simeq (1.8881 \ \underline{/-88.86^\circ}\ )\,\frac{\omega_o^2}{GB} \qquad (7.9.2)$$

Then, the UFR is

$$\omega_{omax} = 0.27GB \qquad (7.9.3)$$

When this filter was built using OAs with GBs around 900KHz, the UFR was found to be twice of that calculated. The better experimental result may be due to the fact that the OAs are mismatched and the mismatching tends to improve the frequency response. If it is assumed that, because of the mismatching of the OAs, the angle in equation 7.9.2 becomes -89.42°, then the UFR increases to 0.52 GB.

vi) Zero Sensitivity:

$$B'_{11} = k_3 \omega'_1 \frac{(s+\omega_2)}{D(s)} \quad , \quad B'_{22} = B'_{33} = 0$$

$$\sum_{i=1}^{3} B'_{ii} = 0.1414\, k_3\, \omega_o \frac{s+\omega_o}{D(s)} = C_z \frac{s-s_{1z}}{D(s)}$$

$$B' = 0.1414\, k_3\, \omega_o \frac{s}{D(s)} = C_B' \frac{s-z_{10}}{D(s)}$$

where

$$C_z = 0.1414\, k_3 \omega_o \quad , \quad s_{1z} = -\omega_o$$

$$C'_B = C_z \quad , \quad z_{10} = 0$$

Using equation 4.4.4,

$$\Delta z_1 = -\omega_L \frac{\omega_o}{GB}$$

The ideal zero moves towards the LHP as ω_o is increased.

vii) ω_o and Q Sensitivities: The calculated and simulated values of the acutal ω_o and Q are listed in Table 7.3.6.

$\frac{\omega_o}{GB}$	$\frac{\Delta p_1}{\omega_o}$	$\frac{p_1}{\omega_o}$	CALCULATED		SIMULATED	
			$\hat{\omega}_o / \omega_o$	$\hat{Q}$	$\hat{\omega}_o / \omega_o$	$\hat{Q}$
10^{-4}	3.76×10^{-6} $-j1.89\times10^{-4}$	-9.996×10^{-3} $+j9.998\times10^{-1}$	0.99986	50.01	0.9998	49.74
10^{-3}	3.76×10^{-5} $-j1.89\times10^{-3}$	-9.962×10^{-3} $+j9.981\times10^{-1}$	0.99816	50.09	0.9981	50.54
10^{-2}	3.76×10^{-4} $-j1.89\times10^{-2}$	-9.624×10^{-3} $+j9.811\times10^{-1}$	0.98117	50.97	0.9816	50.86
10^{-1}	3.76×10^{-3} $-j1.89\times10^{-1}$	-6.244×10^{-3} $+j8.112\times10^{-1}$	0.81125	64.97	0.8506	67.51

Table 7.3.6 OR-MB BP Filter with $H_o = 1$ and Q = 50

viii) Comments: Compared to the MB filter, OR-MB filter has much better HFS and Q sensitivity. The price paid for this improvement is a higher ω_o sensitivity.

VIII. CONCLUSION

8.1 Summary of Results

Analysis and design of networks containing multiple OAs and OTAs using beta matrices is introduced in this dissertation. Networks containing OAs are emphasized, since OAs are presently used more than OTAs.

A systematic method to determine the voltage gain, input and output impedance expressions is presented. The system equations, in matrix form, are used to derive these expressions. In most cases, these equations can be obtained by inspection.

The system equations are also used for stability and sensitivity calculations. For stability, in addition to the general eigenvalue methods, a quick test, HFS test, is also provided. This test yields a necessary but not sufficient criterion which must be satisfied by the OAs in the network.

Another measure of performance, besides stability, is the sensitivity of the network. Active sensitivities of the poles and zeros of the ideal gain are considered. In most applications, the ideal poles move towards the RHP. Using the pole sensitivities, the design frequency at which the network becomes unstable can be approximated. This point is demonstrated in the applications chapter.

Generation of a set of new networks from a given network is also considered. Although, all the configurations obtained by network generation have the same ideal gain, they may have different non-ideal performances.

Thus, some of these networks may be preferred over the others.

The methods developed for n-OA networks in Chapter 2 are adapted to n-OTA networks. Stability and sensitivity considerations are also discussed.

Finally, the methods developed in this dissertation are applied to active filters. It is seen that the stability and sensitivity performance of these networks can easily be determined and in some cases can be improved. Some configurations may inherently have better performance, but in general a trade off exists between the stability and sensitivity of a given configuration.

8.2 Topics for Future Research

A list of topics for future research, for which this dissertation can provide a basis, is given below:

a) The results obtained can be extended to multiple-input-multiple-output networks.
b) Networks employing active feedback can be analyzed.
c) In addition to the voltage gain, the expressions for current, transimpedance, and transadmittance gains can be considered.
d) The magnitude and phase sensitivity expressions can also be derived.
e) With a better modelling of the OTA, a more detailed stability and sensitivity analysis for n-OTA networks can be developed.
f) Methods developed for OAs and OTAs can be extended to include the analysis of networks containing transistors.

g) Methods developed for linear networks can be revised to analyze sampled networks like Switched-Capacitor networks.

h) A CAD package can be developed to generate networks, and calculate the sensitivity and stability performance for each of the generated network.

REFERENCES

[1] Micro-Electronic Circuits, A.S. Sedra and K.C. Smith, HRW, New York, 1982.

[2] S. Rosenstark, "A simplified method of feedback amplifier analysis", IEEE Trans. Education, vol. E-17, No. 4, pp. 192-198, November, 1974.

[3] A.M. Davis, "A general method for analyzing feedback amplifiers", IEEE Trans. Education, vol. E-24, No. 4, pp. 291-293, November, 1981.

[4] S. Esmelioglu and G.M. Wierzba, "Operational amplifier feedback analysis using beta networks", Proc. 25th Midwest Symposium on Circuits and Systems, Houghton, MI, pp. 489-493, August, 1982.

[5] C. Ho, A.E. Ruehli, and P.A. Brennan, "The modified nodal approach to network analysis", IEEE Trans. Circuits and Systems, vol. CAS-22, pp. 504-509, June, 1975.

[6] G. Wilson, "A systematic procedure for the analysis of circuits containing operational amplifiers", IEEE Trans. Education, vol. E-26, No. 3, pp. 99-103, August, 1983.

[7] R.L. Geiger and A. Budak, "Active filters with zero amplifier sensitivity", IEEE Trans. Circuits and Systems, vol. CAS-26, No. 4, pp. 277-288, April, 1979.

[8] S. Esmelioglu, "Analysis and design of feedback amplifiers using beta networks", M.S. Thesis, University of South Carolina, August, 1982.

[9] C. Chen, "Stability of linear multivariable feedback systems", Proc. IEEE, vol. 56, No. 5, pp. 821-828, May, 1968.

[10] C. Chen, "A proof of the stability of multivariable feedback systems", Proc. IEEE, vol. 56, p. 2061, November, 1968.

[11] A.G.J. MacFarlane, "A survey of some recent results in linear multivariable feedback theory", Automatica, vol. 8, pp. 455-492, 1972.

[12] A.G.J. MacFarlane, "Return-difference and return-ratio matrices and their use in analysis and design of multivariable feedback control systems", Proc. IEE, vol. 117, No. 10, pp. 2037-2049, October, 1970.

[13] H.H. Rosensbrock, "Design of multivariable control systems using the Inverse Nyquist Array", Proc. IEE, vol. 116, No. 11, pp. 1929-1936, November, 1969.

[14] F. Fallside and H. Seraji, "Design of optimal systems by a frequency domain technique", Proc. IEE, vol. 117, No. 10, pp. 2017-2024, October, 1970.

[15] R.L. Geiger, "Parasitic pole approximation techniques for active filter design", Trans. Circuits and Systems, vol. CAS-27, No. 9, pp. 793-799, September, 1980.

[16] G. Wilson, Y. Bedri, and P. Bowron, "RC-Active networks with reduced sensitivity to amplifier gain-bandwidth product", IEEE Trans. Circuits and Systems, vol. CAS-21, No. 5, pp. 618-626, September, 1974.

[17] R. Mackay and A.S. Sedra, "Generation of low sensitivity state-space active filters", IEEE Trans. Circuits and Systems, vol. CAS-27, No. 10, pp. 863-870, October, 1980.

[18] W.B. Mikhael and B.B. Bhattacharyya, "A practical design for insensitive RC-active filters", Trans. Circuits and Systems, vol. CAS-22, pp. 407-415, May, 1975.

[19] R.L. Geiger and A. Budak, "Design of active filters independent of first- and second-order operational amplifier time constant effects", IEEE Trans. Circuits and Systems, vol. CAS-28, No. 8, pp. 749-757, August, 1981.

[20] A. Antoniou, "New gyrator circuits obtained by using nullors", Electronic Letters, vol. 4, No. 5, pp. 87-88, March, 1968.

[21] R. Palomera-Garcia, "Generation of active RC-circuits by the nullor equivalency concept", Proc. European Conference on Circuit Theory and Design", pp. 53-57, 1978.

[22] G.M. Wierzba and S.C. Stewart, "The theory and application of op-amp relocation", Proc. 14th Southeastern Symposium on System Theory, Blacksburg, VA, pp. 97-100, April, 1982.

[23] H.S. Malvar, "Electronically controlled active-C filters and equalizers with operational transconductance amplifiers", IEEE Trans. Circuits and Systems, vol. CAS-31, No. 7, pp. 645-649, July, 1984.

[24] R.L. Geiger and J. Ferrel, "Voltage controlled filter design using operational transconductance amplifiers", Proc. IEEE/ISCAS, pp. 594-597, May, 1983.

[25] R.L. Geiger and E.S. Sinencio, "Active filter design using operational transconductance amplifiers: A tutorial", IEEE Circuits and Devices Magazine, vol. 1, No. 2, pp. 20-32, March, 1985.

[26] W.J. Kerwin, L.P. Huelsman, and R.W. Newcomb, "State variable synthesis for insensitive integrated circuit transfer functions", IEEE J. Solid-State Circuits, vol. SC-2, pp. 87-92, September, 1967.

[27] A. Antoniou, "Realization of gyrators using operational amplifiers and their use in RC-active network synthesis", Proc. IEE, pp. 1838-1850, November, 1979.

[28] Elementary Matrix Algebra, F.E. Hohn, 2nd ed., The MacMillan Co., New York, 1964.

[29] Introduction to Matrix Computations, G.W. Stewart, Academic Press, Florida, 1973.

[30] Fundamentals of Complex Analysis, E.B. Saff and A.D. Snider, Prentice-Hall, New Jersey, 1976.

[31] Automatic Control Systems, B.C. Kuo, 4th ed., Prentice-Hall, New Jersey, 1982.

[32] Introduction to Linear Algebra, L.W. Johnson and R.D. Riess, Addison-Wesley, Massachusetts, 1981.

[33] Modern Filter Design, M.S. Ghausi and K.R. Laker, Prentice-Hall, New Jersey, 1981.

[34] L. Brown and A.S. Sedra, "New mulifunction filter circuit with inherently stable Q-factor," Electronic Letters, Vol. 13, pp. 719-721, October, 1977.